Why Do All Those Damned Detectors Look The Same?

Jim Thomas

Lawrence Berkeley Laboratory

January 11, 2004

ATLAS vs PHENIX vs ….

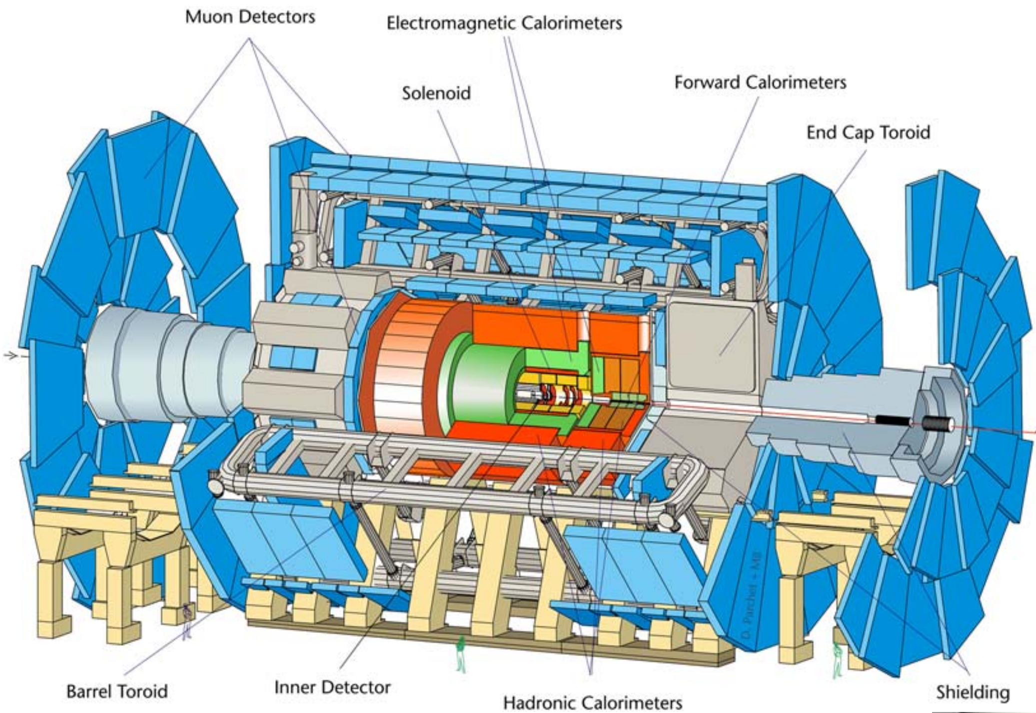

ATLAS

They are about the same size

They are about the same shape

Are they really different?

Even fixed target detectors look like an angular slice of one of these detectors

PHENIX

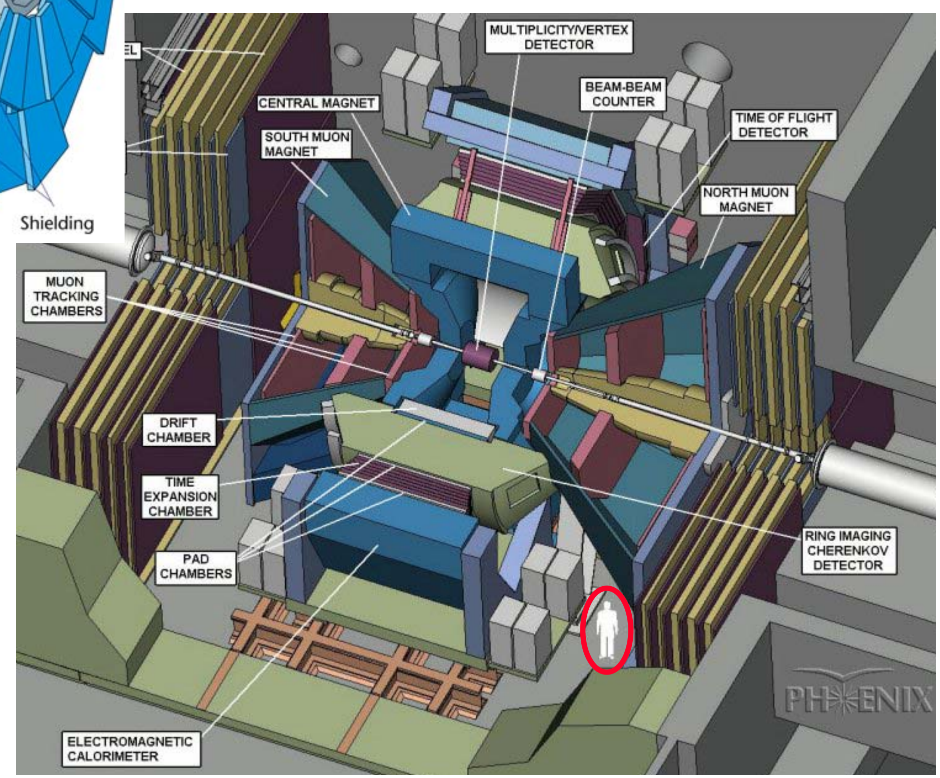

References

Outstanding References

- **Particle Properties Data Booklet**
  - **Particle properties**
  - **Excellent summaries of particle detection techniques**
  - **http://pdg.lbl.gov to view the pages or order your own copy**

- **Sauli's lecture notes on wire chambers (CERN 77-09)**

- **W. Blum and L. Rolandi, "Particle Detection with Drift Chambers", Springer, 1994.**

This talk relies heavily on additional resources from the Web

- **C. Joram – CERN Summer Student Lectures 2003**
- **T.S. Verdee – SUSSP 2003**
- **S. Stapnes – CERN School of Phyics 2002**

The Oldest Particle Detector – and a good one, too.

- **High sensitivity to photons**
- **Good spatial resolution**
- **Large dynamic range 1:10^{14}**
- **(Once upon a time) Used to tune cyclotron beams via scintillation light**

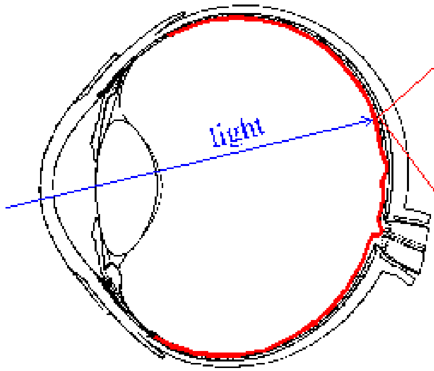

Adapted from Boycott & Dowling, 1969

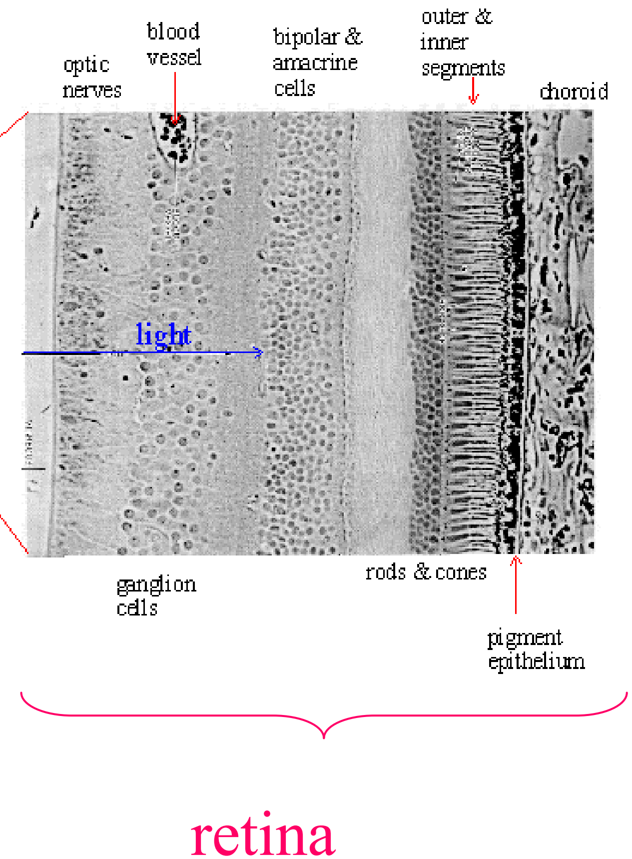

What should a particle detector do?

J. Plücker 1858 ➠ J.J. Thomson 1897

Fig. 2.

Thomson’s cathode ray tube

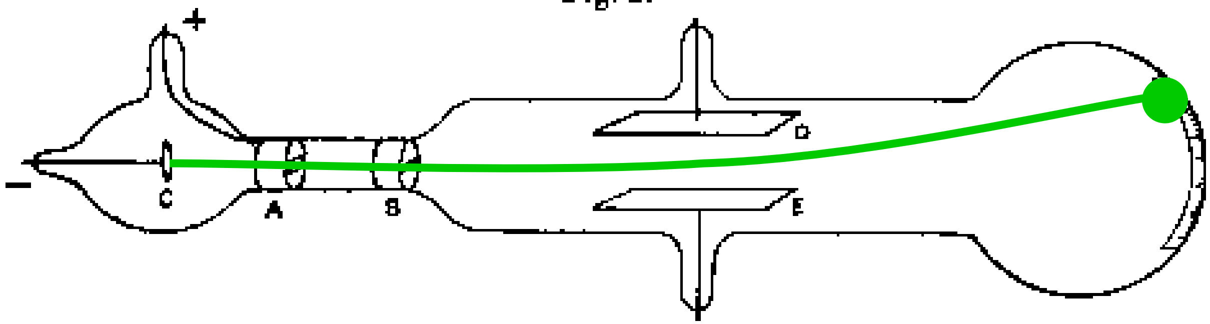

accelerator

manipulation
By E or B field

detector

- **Note the scale pasted on the outside of the tube!**
- **Glass scintillates and we “see” the effect on the electron beam**
- **Today … mean pt is 500 MeV so we need a meter of steel and concrete to stop the particle and make a total energy measurement.**

First electrical signal from a particle

E. Rutherford

1909

H. Geiger

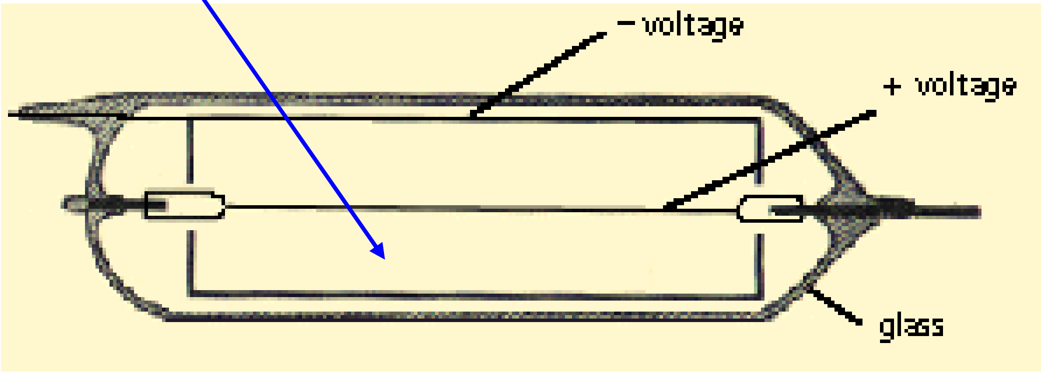

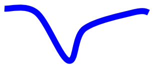

The Geiger counter

First tracking detector

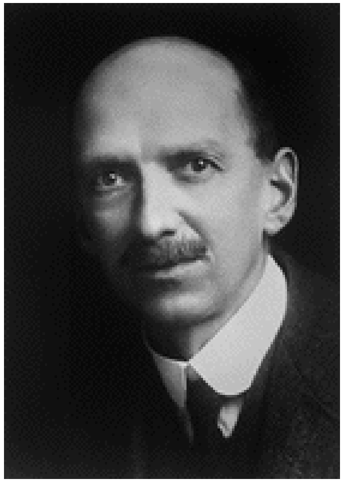

C. T. R. Wilson, 1912, Cloud chamber

The general procedure was to allow water to evaporate in an enclosed container to the point of saturation and then lower the pressure, producing a super-saturated volume of air. Then the passage of a charged particle would condense the vapor into tiny droplets, producing a visible trail marking the particle's path.

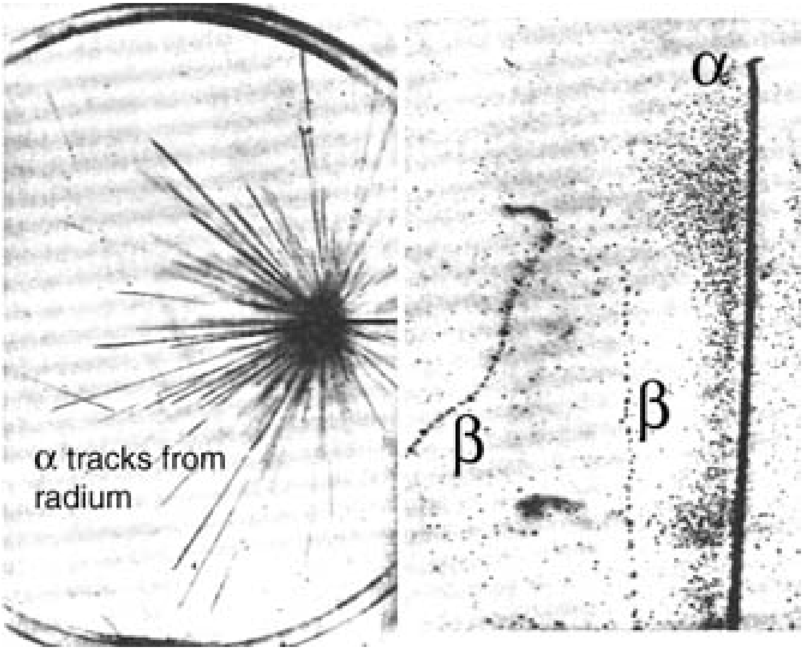

Detector Philosophy

- Particles are detected by their interaction with matter
- Many different physical principals are involved
  - Electromagnetic
  - Weak
  - Strong
  - Gravity
- Most detection techniques rely on the EM interaction
  - Although, all four fundamental forces are used to measure and detect particles
- Ultimately, we observe ionization and excitation of matter.
  In this day and age, it always ends up as an electronic signal.

Coulomb Scattering

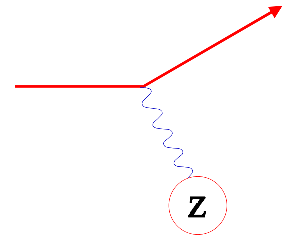

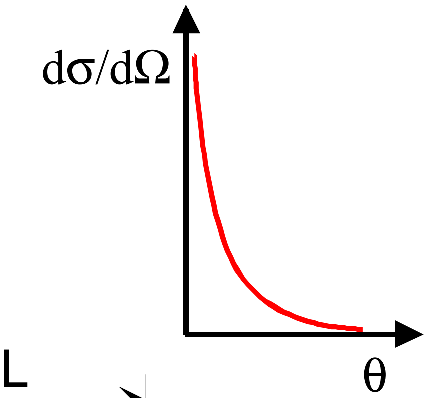

An incoming particle with charge **z** interacts with a target of nuclear charge **Z**. The cross-section for this e.m. process is

$$\frac{d\sigma}{d\Omega} = 4zZr_e^2\left(\frac{m_e c}{\beta p}\right)^2 \frac{1}{\sin^4\theta/2}$$

Rutherford formula

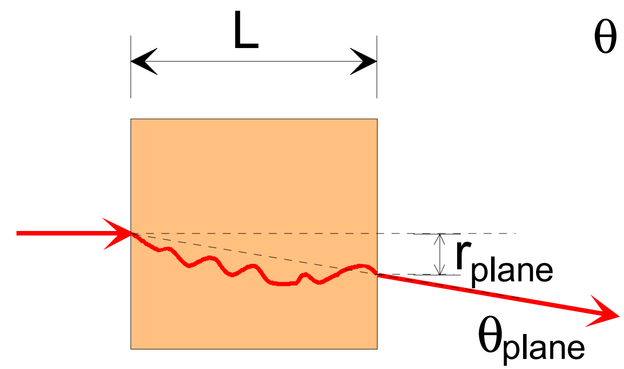

Average scattering angle $<\theta> = 0$

Cross-section for $\theta \rightarrow 0$ is infinite !

This implies that there will be many soft scattering events.

Multiple Coulomb Scattering

In sufficiently thick material layer → the particle will undergo multiple scattering. There will be angular deflections and energy loss.

$$\theta_0 \approx \frac{13.6MeV}{\beta\, c\, p} z \sqrt{\frac{x}{X_0}}\left[1 + 0.20\ \ln(x/X_0)\right]$$

Radiation Length

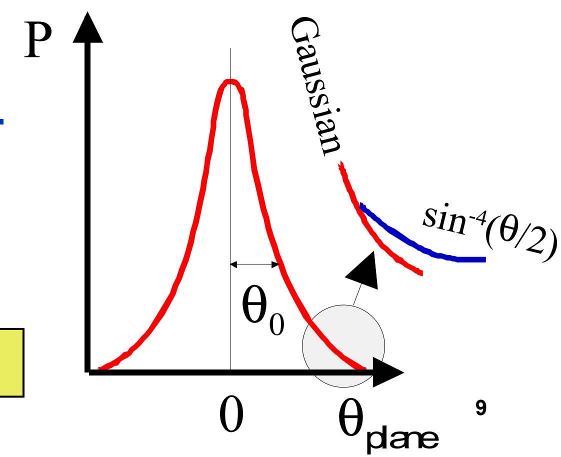

How do particles lose energy in matter?

$$\left\langle \frac{dE}{dx} \right\rangle = -\int_0^\infty NE \frac{d\sigma}{dE} \hbar \, d\omega$$

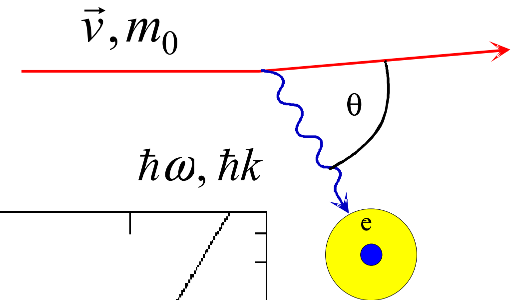

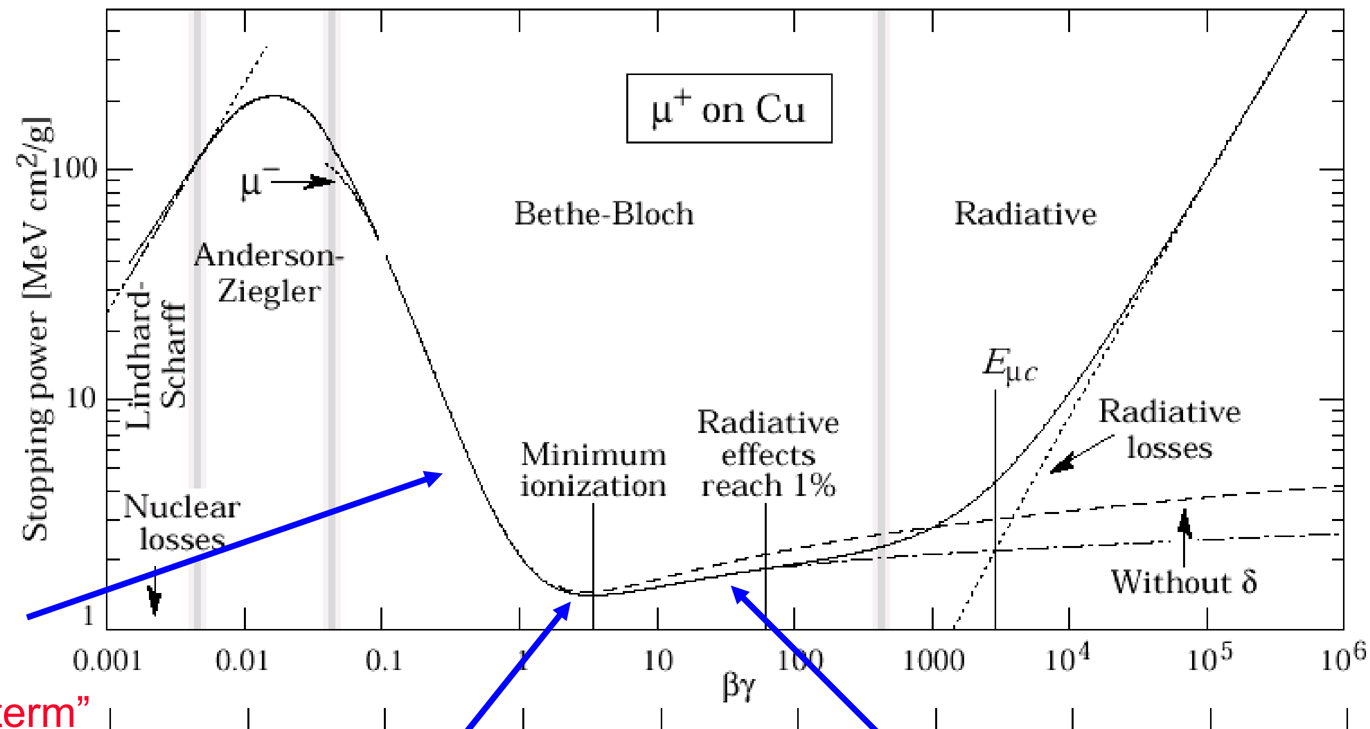

$$\left\langle \frac{dE}{dx} \right\rangle \propto \frac{1}{\beta^2}$$

"kinematic term"

"minimum ionizing particles" $\beta\gamma \approx$ 3-4

"relativistic rise" $\left\langle \frac{dE}{dx} \right\rangle \propto \ln \beta^2\gamma^2$

Bethe-Bloch Formula

$$\left\langle \frac{dE}{dx} \right\rangle = -4\pi N_A r_e^2 m_e c^2 z^2 \frac{Z}{A} \frac{1}{\beta^2} \left[\ln\left(\frac{2m_e c^2 \gamma^2 \beta^2}{I} \right) - \beta^2 - \frac{\delta}{2} \right]$$

density effect

ionization constant

dE/dx depends on β

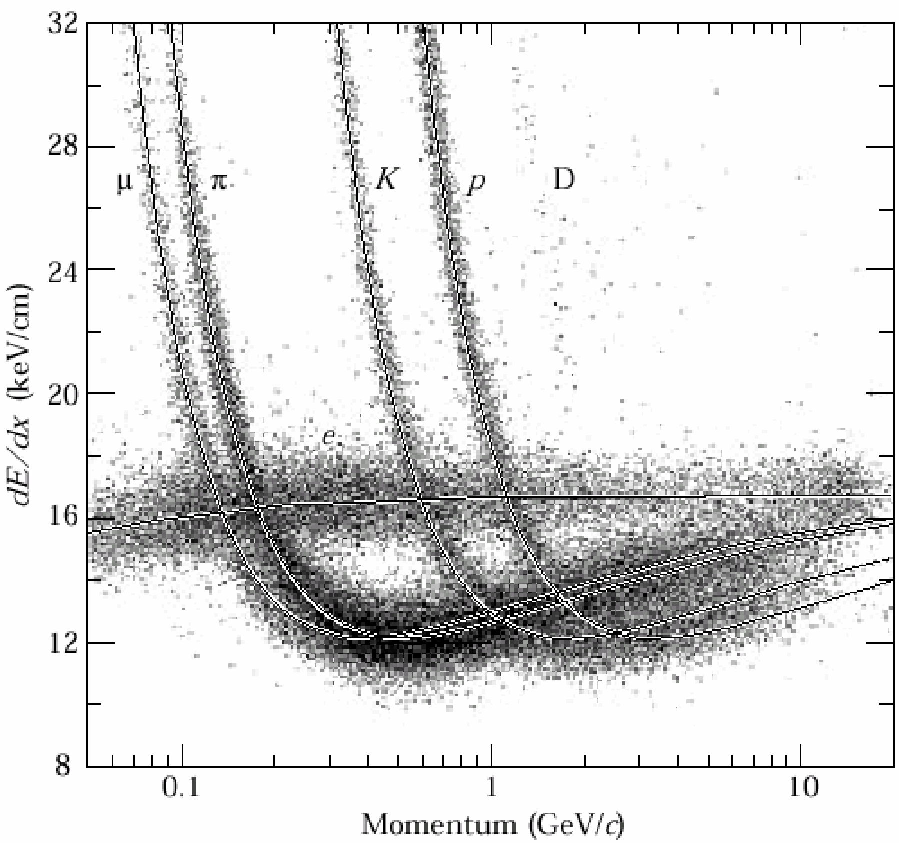

Pep 4 TPC

- dE/dx depends only on β and is independent of mass
- Particles with different masses have different momenta (for same β)
- dE/dx in [MeV $g^{-1}cm^2$]
  - in a gas detector this gets shortened to keV/cm.
- First approximation: medium characterized by electron density, N ~ Z/A.

Landau tails

Real detectors (limited granularity) can not measure <dE/dx> .
They measure the energy ΔE deposited in a layer of finite thickness δx.

For thin layers → Few collisions, some with high energy transfer.

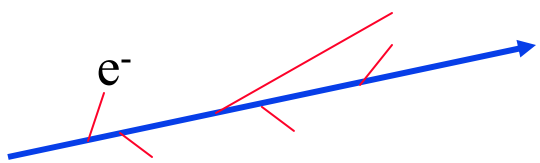

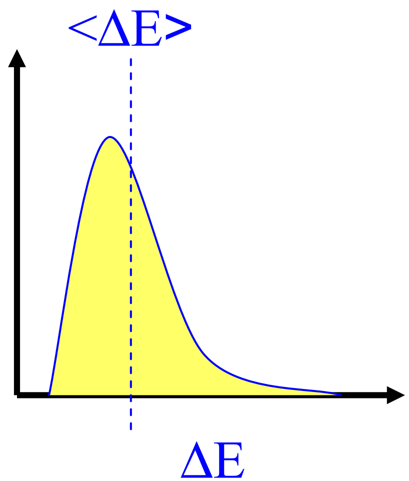

→ Energy loss distributions show large fluctuations towards high losses: "<u>Landau tails</u>" due to "<u>δ electrons</u>"

For thick layers and high density materials → Many collisions → Central Limit Theorem → Gaussian shape distributions.

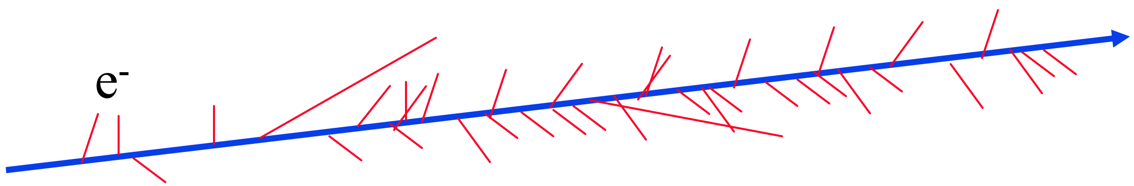

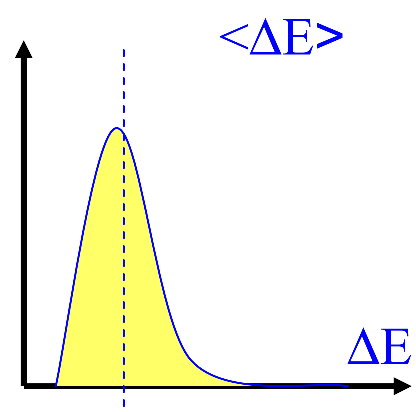

Ionization of gases

Fast charged particles ionize the atoms of a gas.

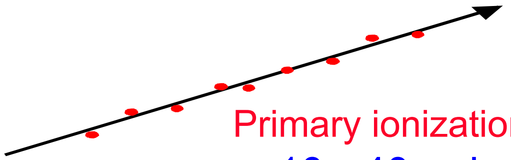

Primary ionization

10 - 40 pairs/cm

ΔE/pair ~ 25 eV

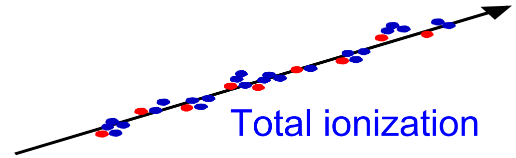

Total ionization

$$n_{total} \approx 3 \ldots 4 \cdot n_{primary}$$

Often the resulting primary electron will have enough kinetic energy to ionize other atoms.

Assume detector, 1 cm thick, filled with Ar gas:

1 cm

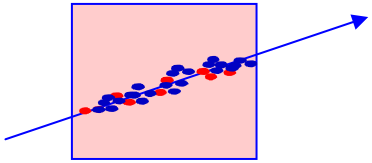

~ 100 e-ion pairs

100 electron-ion pairs are not easy to detect!

Noise of amplifier $\approx$ 1000 e$^-$ (ENC) !

We need to increase the number of e-ion pairs.

Gas Amplification in a Proportional Counter

Consider cylindrical field geometry (simplest case):

$$E(r) = \frac{CV_0}{2\pi\varepsilon_0} \cdot \frac{1}{r}$$

$$V(r) = \frac{CV_0}{2\pi\varepsilon_0} \cdot \ln\frac{r}{a}$$

C = capacitance / unit length

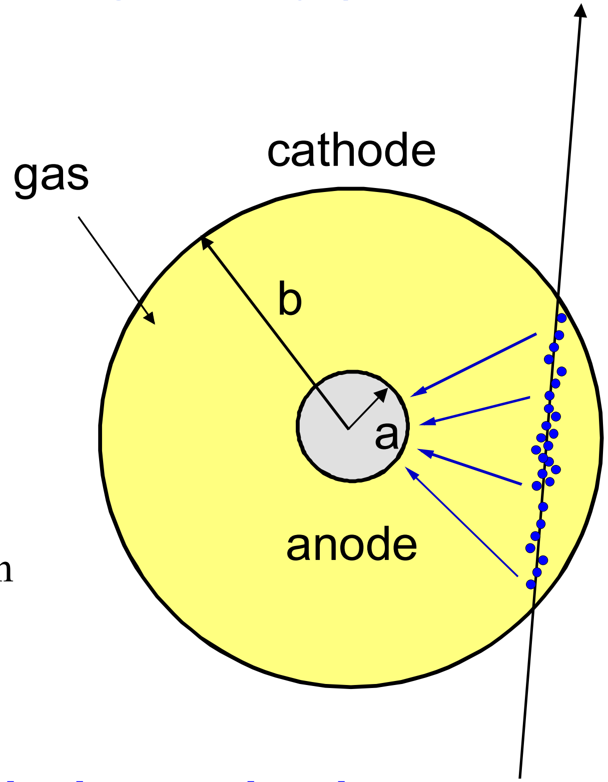

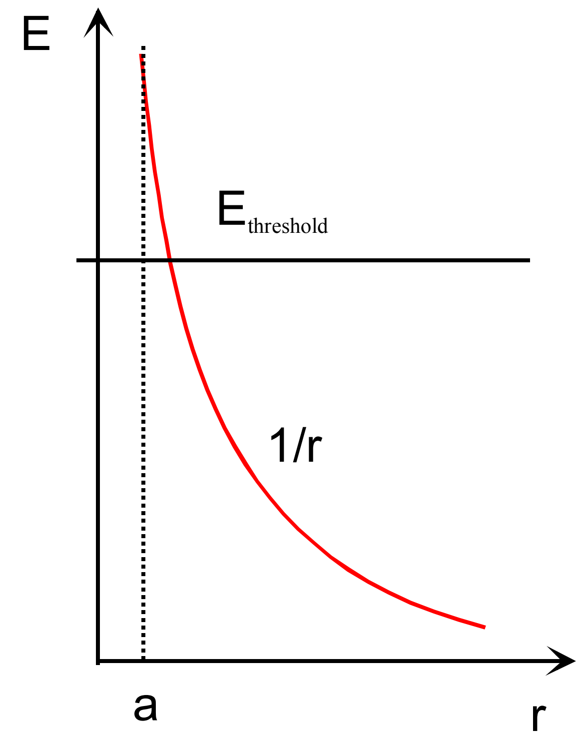

Electrons drift towards the anode wire

Close to the anode wire the electric field is sufficiently high (kV/cm), that the e$^-$ gain enough energy for further ionization $\rightarrow$ <u>exponential increase</u> in the number of e$^-$-ion pairs.

Signal Formation - Proportional Counter

Avalanche form within a few radii or the wire and within t < 1 ns!

Signal induction both on anode and cathode due to moving charges (both electrons and ions).

$$dv = \frac{Q}{lCV_0}\frac{dV}{dr}dr$$

(F. Sauli, CERN 77-09)

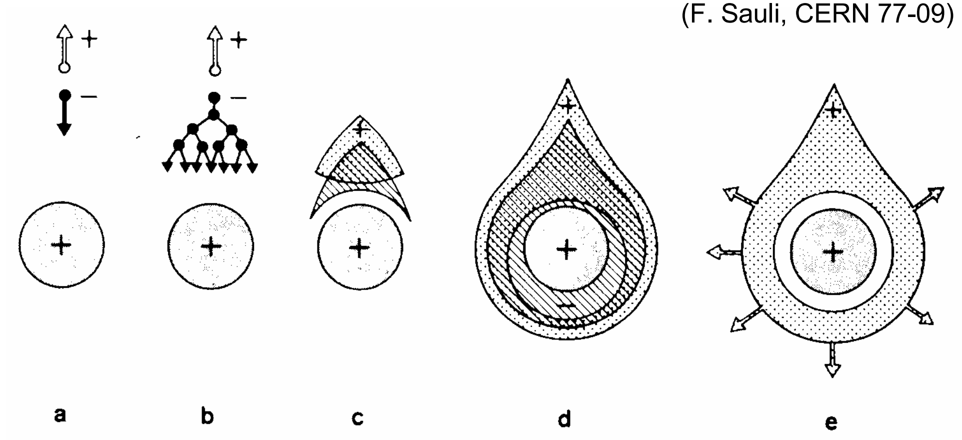

Electrons are collected on the anode wire, (i.e. *dr* is small, only a few µm). Electrons contribute only very little to detected signal (few %).

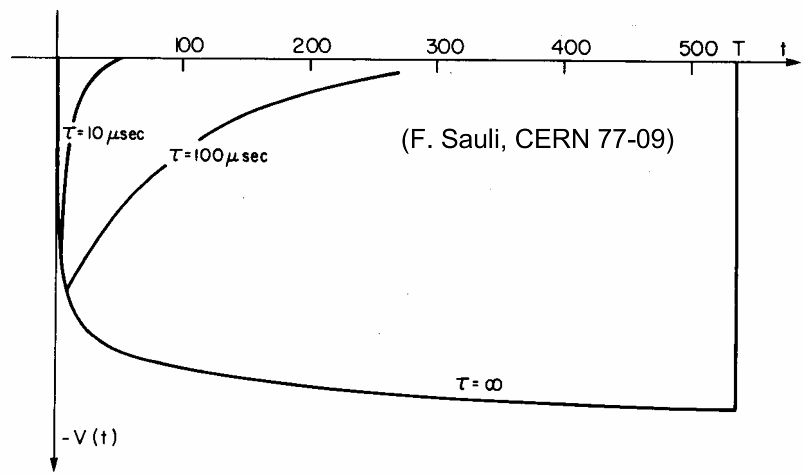

(F. Sauli, CERN 77-09)

Ions have to drift back to cathode, i.e. *dr* is big. Signal duration limited by total ion drift time !

We need electronic signal differentiation to limit dead time.

Multiwire Proportional Chamber

Multi wire proportional chamber (MWPC)

(G. Charpak et al. 1968, Nobel prize 1992)

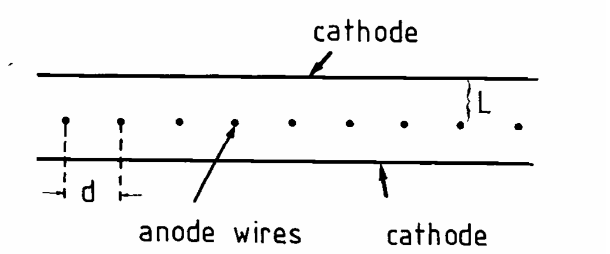

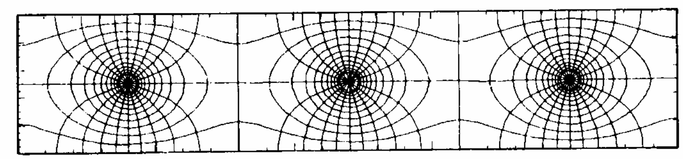

field lines and equipotentials around anode wires

Address of fired wire(s) only give 1-dimensional information. This is sometimes called "Projective Geometry". It would be better to have a second dimension ….

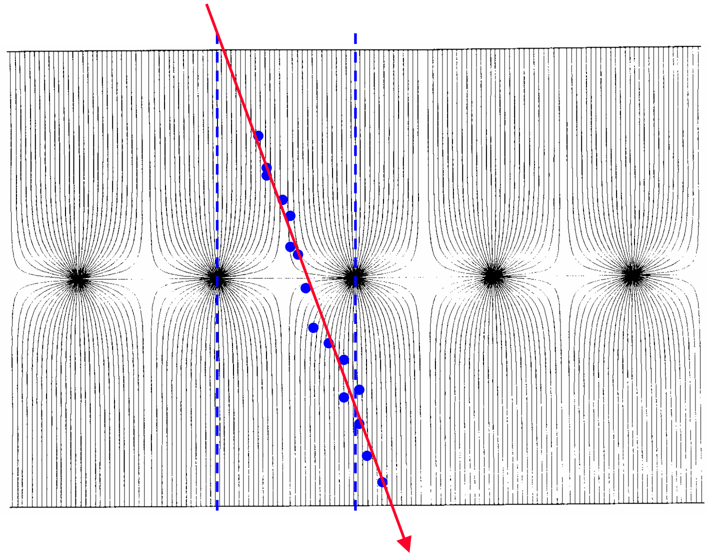

Typical parameters:

L = 5mm, d = 1mm, r_{wire}= 20μm.

Normally digital readout:
spatial resolution limited to

$$\sigma_x \approx \frac{d}{\sqrt{12}}$$

(d=1mm, σ_x=300 μm)

The Second Dimension … 2D readout

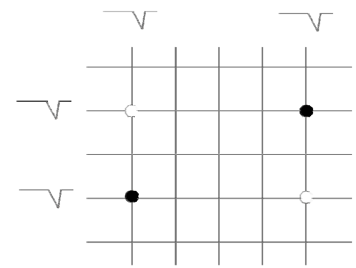

Crossed wire planes. Ghost hits. Restricted to low multiplicities.
90 degrees or stereo planes crossing at small angle.

Charge division: Resistive wires (Carbon,2kΩ/m).

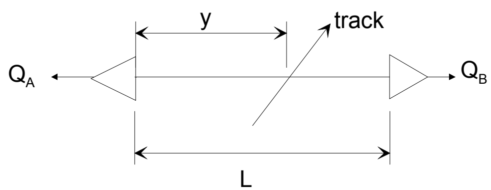

$$\frac{y}{L} = \frac{Q_B}{Q_A + Q_B} \qquad \sigma\left(\frac{y}{L}\right) \text{ up to } 0.4\%$$

Timing difference:

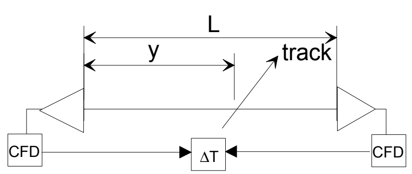

$$\sigma(\Delta T) = 100\,ps$$
$$\rightarrow \ \sigma(y) \approx \textit{few cm}$$

Segmented cathode planes:

Analog readout of cathode planes $\rightarrow \sigma \approx 100\ \mu m$

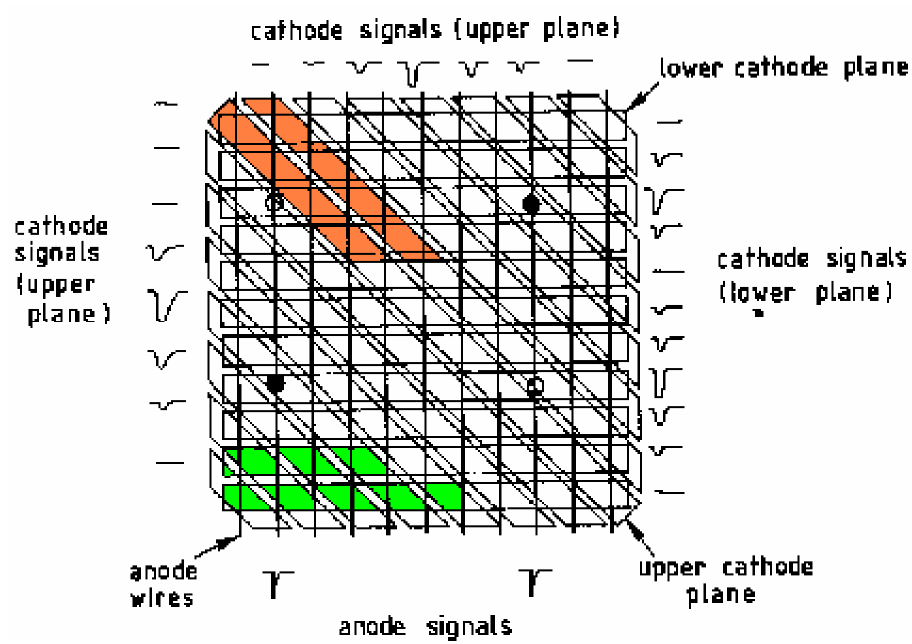

Timing Difference: Drift Chambers

Drift Chambers :

- **Reduced numbers of readout channels**
- **Distance between wires typically 5-10cm giving around 1-2 μs drift-time**
- **Resolution of 50-100μm achieved limited by field uniformity and diffusion**
- **Perhaps problems with occupancy of tracks in one cell.**

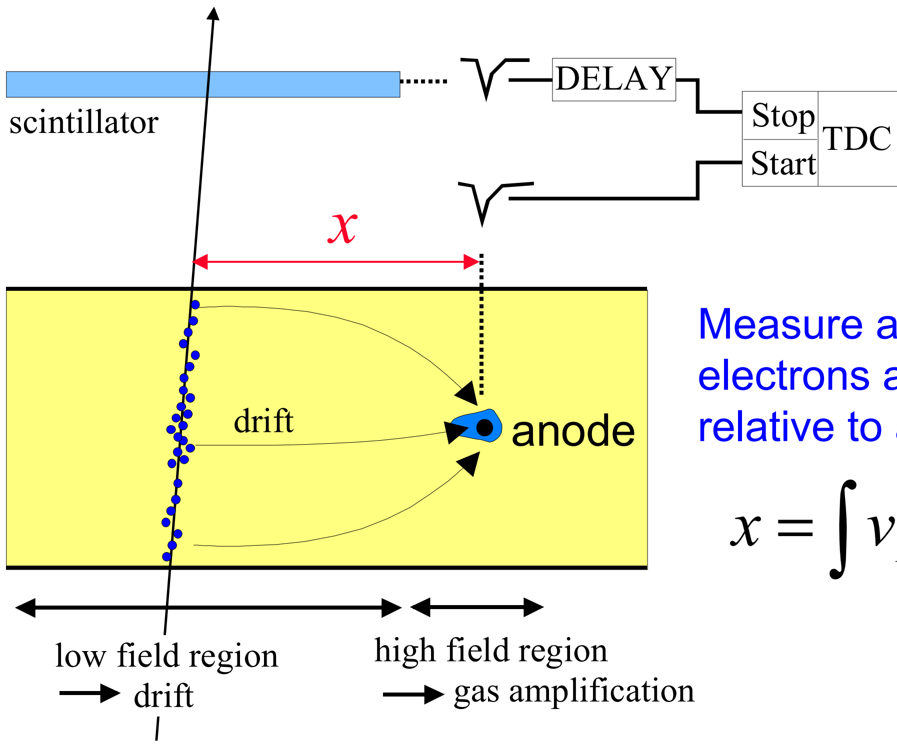

Measure arrival time of electrons at sense wire relative to a time t_0.

$$x = \int v_D(t)\,dt$$

(First studies: T. Bressani, G. Charpak, D. Rahm, C. Zupancic, 1969
First operation drift chamber: A.H. Walenta, J. Heintze, B. Schürlein, NIM 92 (1971) 373)

Drift Chambers: Many Possible Designs

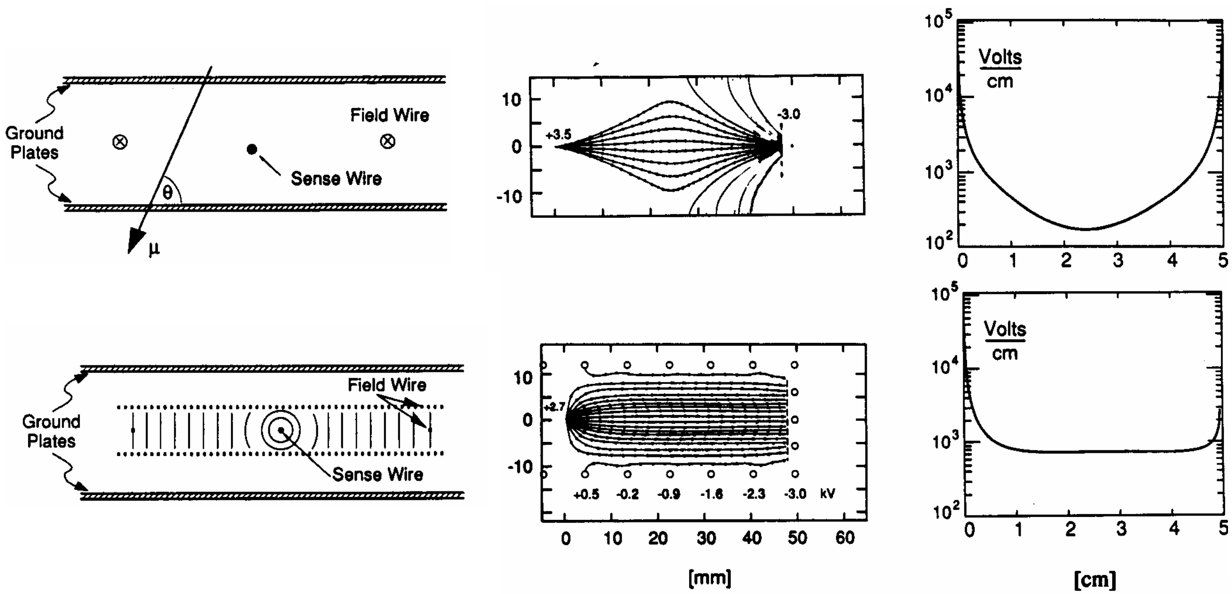

(U. Becker, in: Instrumentation in High Energy Physics, World Scientific)

- What happens during the drift towards the anode wire?
  - We need to know the drift velocity
  - Diffusion, too.

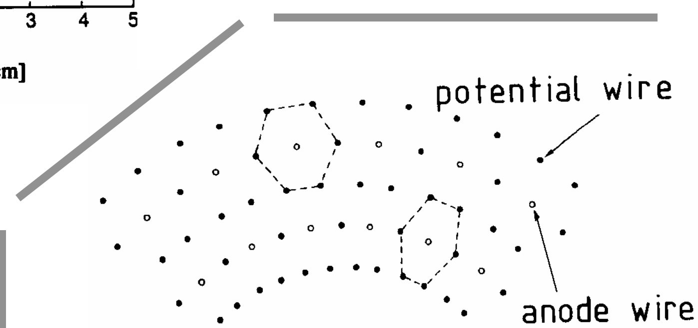

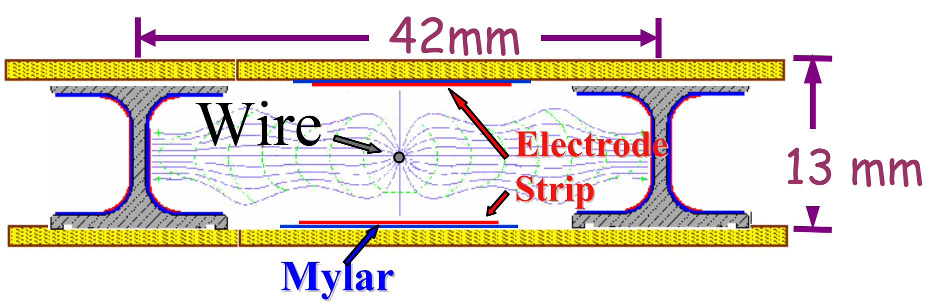

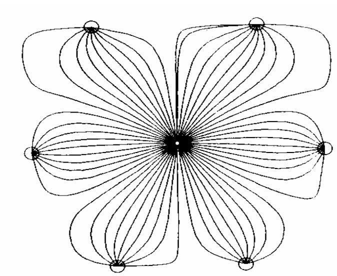

Drift and Diffussion in Gases

Without external fields:

Electrons and ions will lose their energy due to collisions with the gas atoms $\rightarrow$ thermalization

$$\varepsilon = \frac{3}{2} kT \approx 40 \text{ meV}$$

Undergoing multiple collisions, a localized ensemble of charges will diffuse

$$\frac{dN}{N} = \frac{1}{\sqrt{4\pi Dt}} e^{-(x^2/4Dt)}\, dx$$

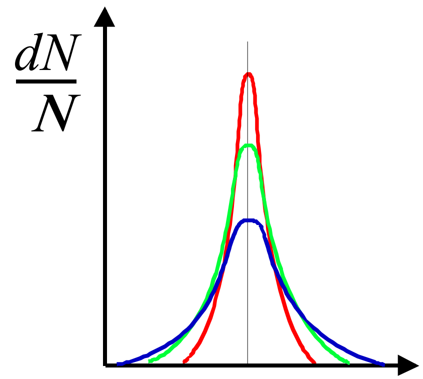

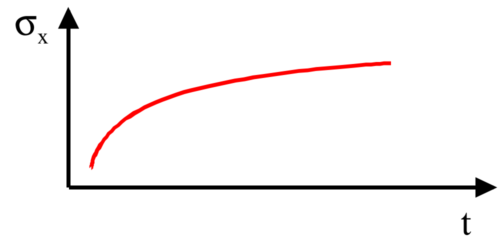

$$\sigma_x(t) = \sqrt{2Dt} \qquad or \quad D = \frac{\sigma_x^2(t)}{2t}$$

D: diffusion coefficient

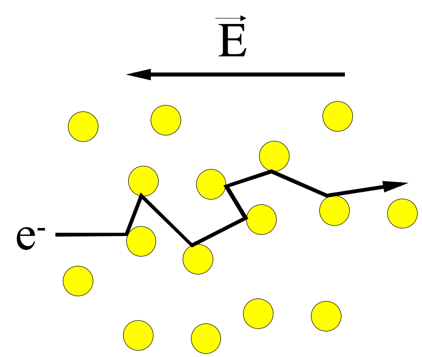

With External electric field:

multiple collisions due to
scattering from gas atoms $\rightarrow$ drift

$$\vec{v}_D = \mu \vec{E} \qquad \mu = \frac{e\tau}{m} \ \text{(mobility)}$$

Typical electron drift velocity: **5 cm/μs**

Ion drift velocities are ~1000 times smaller

3D: The Time Projection Chamber

Time Projection Chamber → full 3-D track reconstruction

- x-y from wires and segmented cathode of MWPC
- z from drift time
- in addition dE/dx information

Diffusion significantly reduced by B-field.

Requires precise knowledge of v_D →
LASER calibration + p,T corrections

Drift over long distances → very good gas quality required

Space charge problem from positive ions, drifting back to midwall → use a gated grid

ALEPH TPC
(ALEPH coll., NIM A 294 (1990) 121,
W. Atwood et. Al, NIM A 306 (1991) 446)

Ø 3.6M, L=4.4 m

ΔV_g = 150 V

$\sigma_{R\phi} = 173\ \mu m$
$\sigma_z = 740\ \mu m$
(isolated leptons)

STAR TPC

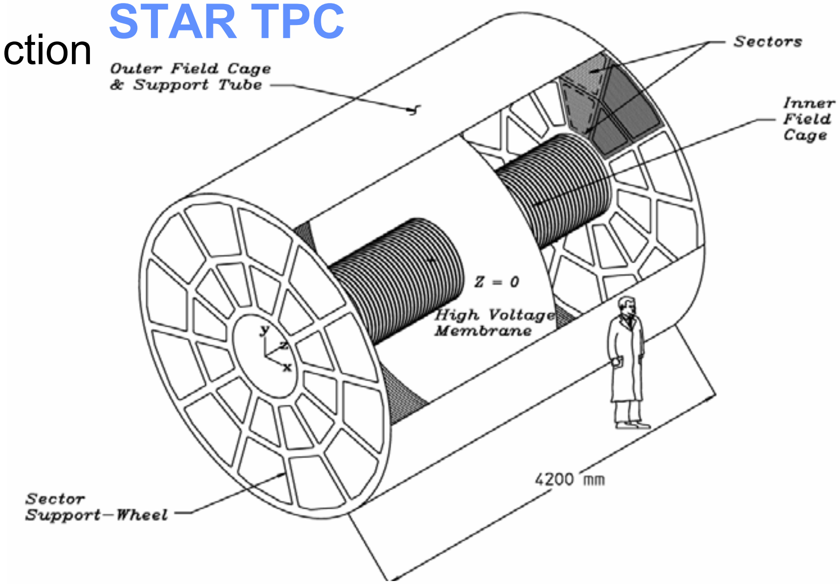

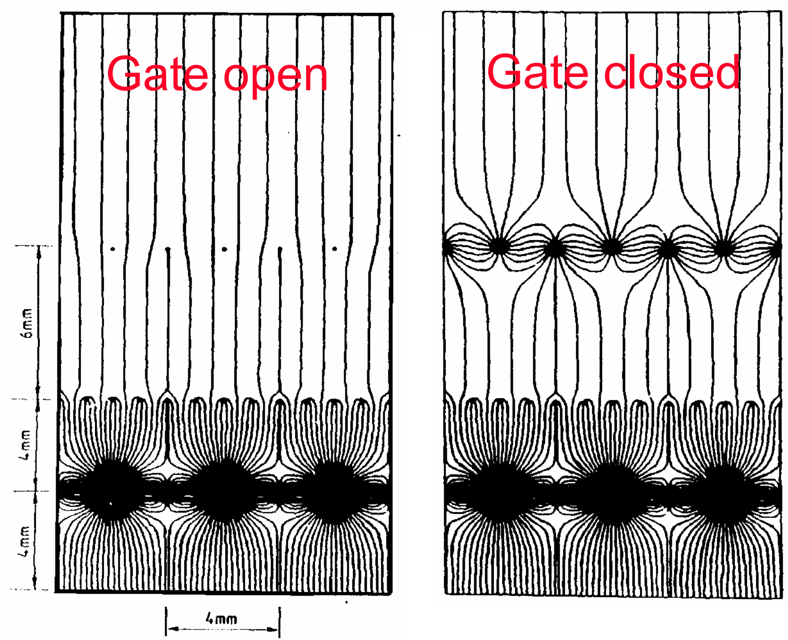

Momentum Measurement in a Uniform Field

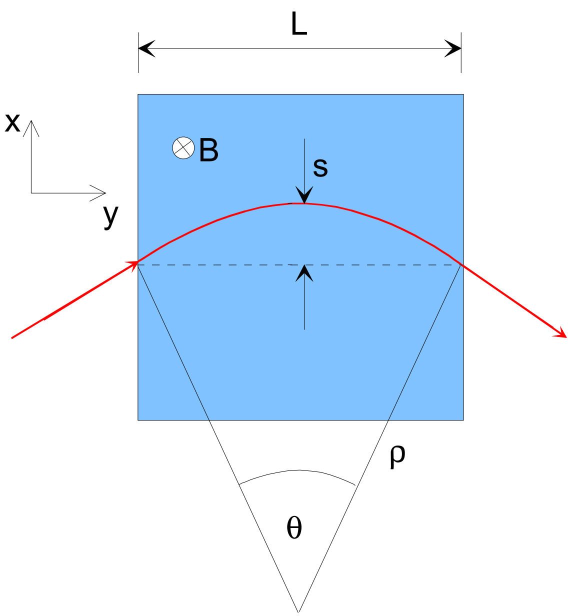

$$\frac{mv^2}{\rho} = q(v \times B) \quad \rightarrow \quad p_T = qB\rho$$

$$\boxed{p_T\ (\mathrm{GeV/c}) = 0.3B\rho \quad (\mathrm{T \cdot m})}$$

$$\frac{L}{2\rho} = \sin\theta/2 \approx \theta/2 \quad \rightarrow \quad \theta \approx \frac{0.3L \cdot B}{p_T}$$

$$s = \rho(1 - \cos\theta/2) \approx \rho\frac{\theta^2}{8} \approx \frac{0.3}{8}\frac{L^2 B}{p_T}$$

The sagitta $s = x_2 - \frac{1}{2}(x_1 + x_3)$ **is determined by 3 measurements with error** $\sigma(x)$**:**

$$\left.\frac{\sigma(p_T)}{p_T}\right|^{meas.} = \frac{\sigma(s)}{s} = \frac{\sqrt{\frac{3}{2}}\,\sigma(x)}{s} = \frac{\sigma(x) \cdot 8p_T}{0.3 \cdot BL^2} \cdot \sqrt{\frac{3}{2}}$$

$$\boxed{\left.\frac{\sigma(p_T)}{p_T}\right|^{meas.} = \frac{\sigma(x) \cdot p_T}{0.3 \cdot BL^2}\sqrt{720/(N+4)} \qquad (N > 10)}$$

Momentum Resolution: the STAR Magnet + TPC

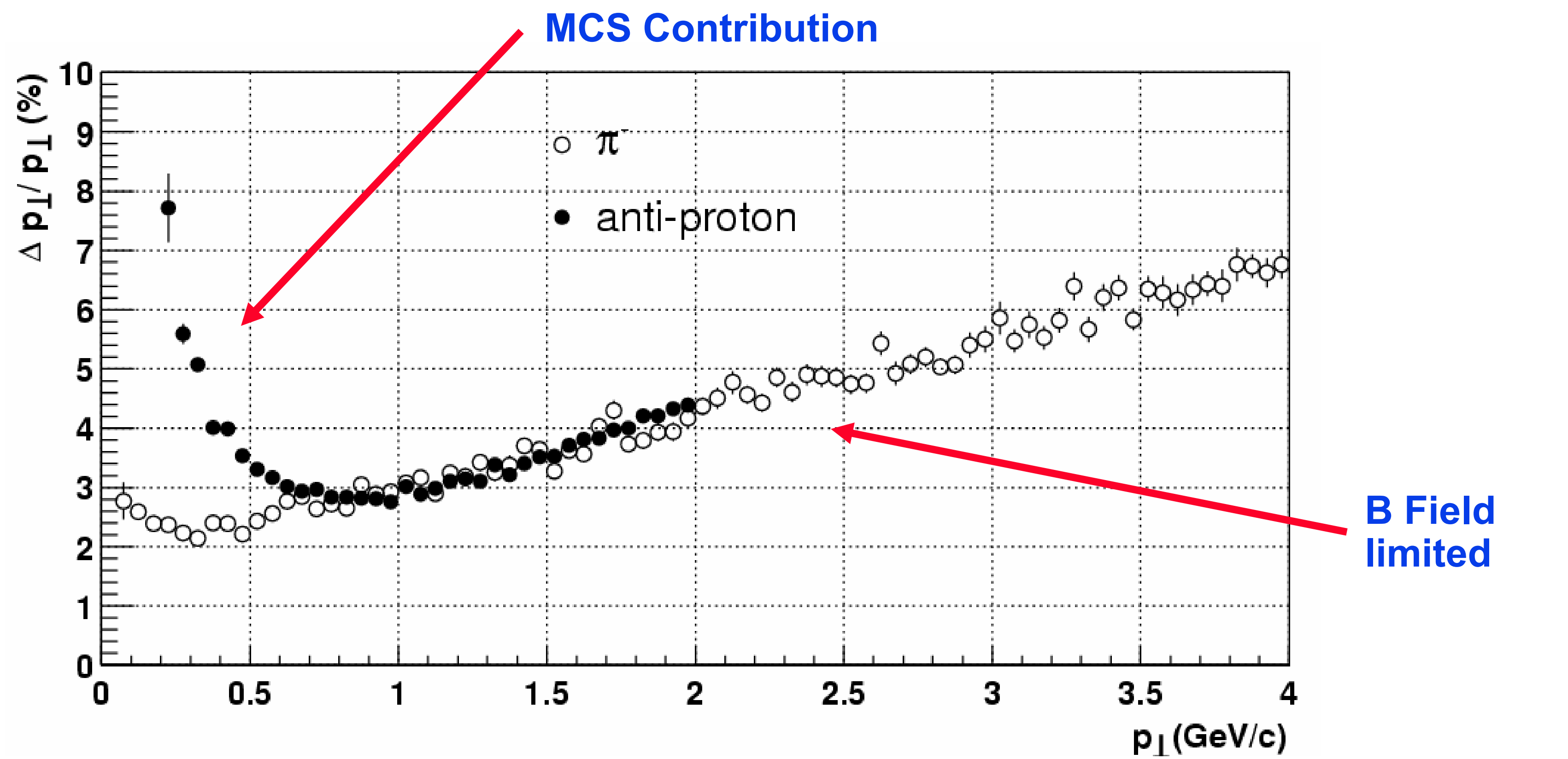

- Momentum resolution is only limited by the strength of the magnetic field and is independent of the mass of the particle at high P_T
- Momentum resolution at low P_T is determined by multiple coulomb scattering (MCS)

Semiconductor Detectors: Silicon

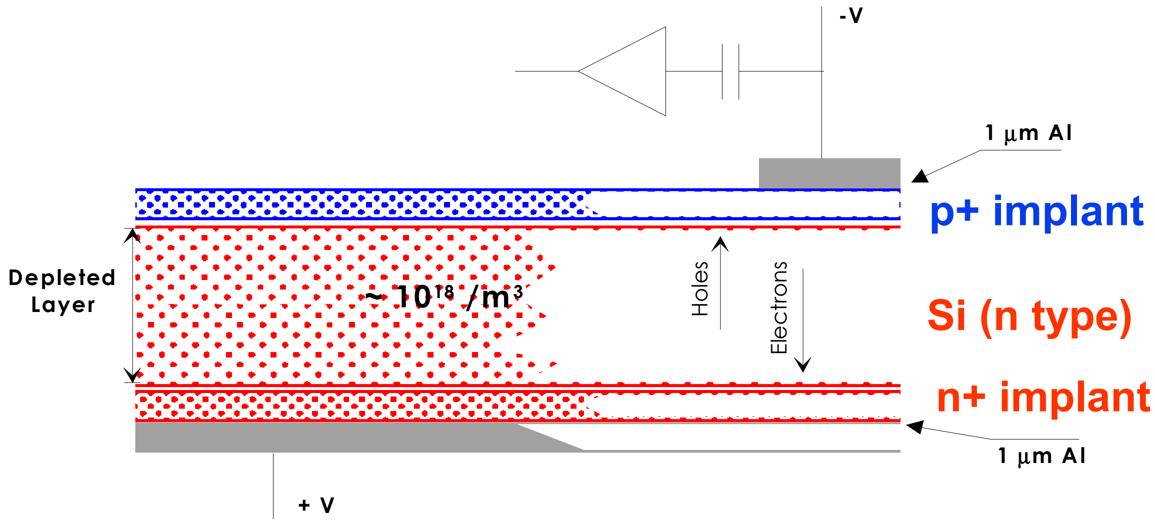

The typical Semiconductor detector is a based on a Si diode structure

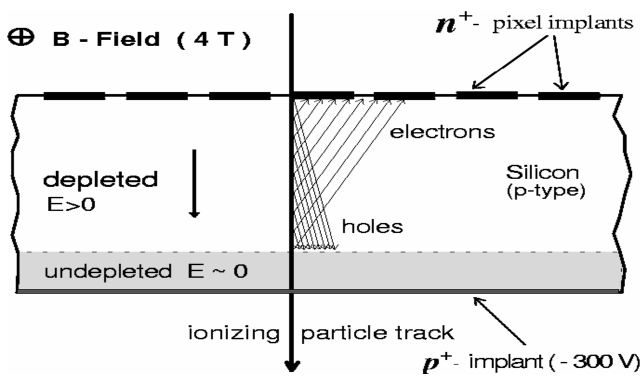

Interaction with ionizing radiation

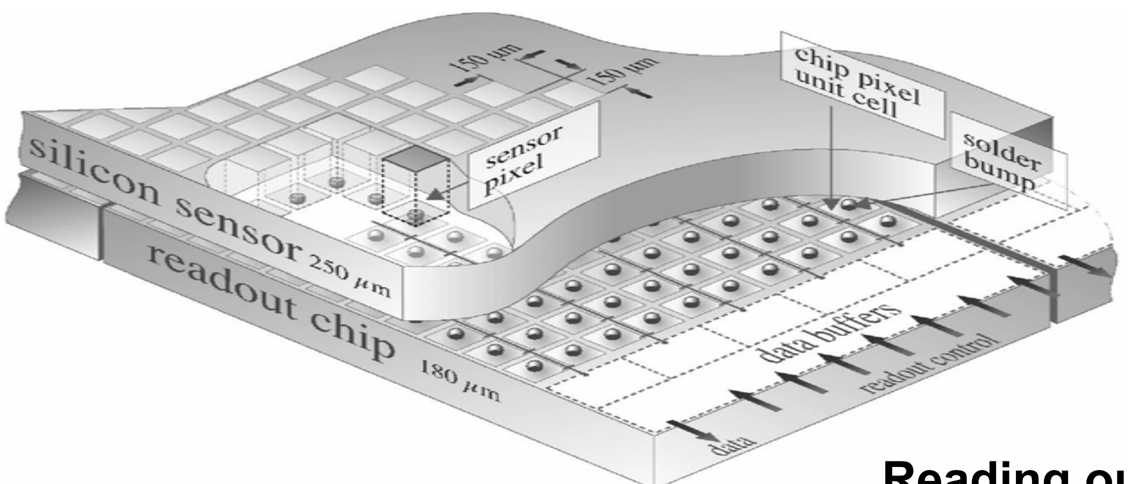

Reading out the pixels

The Properties of Silicon

Some characteristic numbers for silicon

- Band gap: E_g =1.12 V.
- E(e^--hole pair) = 3.6 eV, (≈ 30 eV for gas detectors).
- High specific density (2.33 g/cm^3) → ΔE/track length for M.I.P.'s.: 390 eV/μm ≈ 108 e-h/ μm (average)
- High mobility: μ_e =1450 cm^2/Vs, μ_h = 450 cm^2/Vs
- Detector production by microelectronic techniques → small dimensions → fast charge collection (<10 ns).
- Rigidity of silicon allows thin self supporting structures. Typical thickness 300 μm → ≈ 3.2 ·10^4 e-h (average)
- But: No charge multiplication mechanism!

- **Si Structures are small and can be mass produced in large arrays**
- **Ideal for locating a point on the track of a particle**

Scintillation Light: Inorganic Scintillators

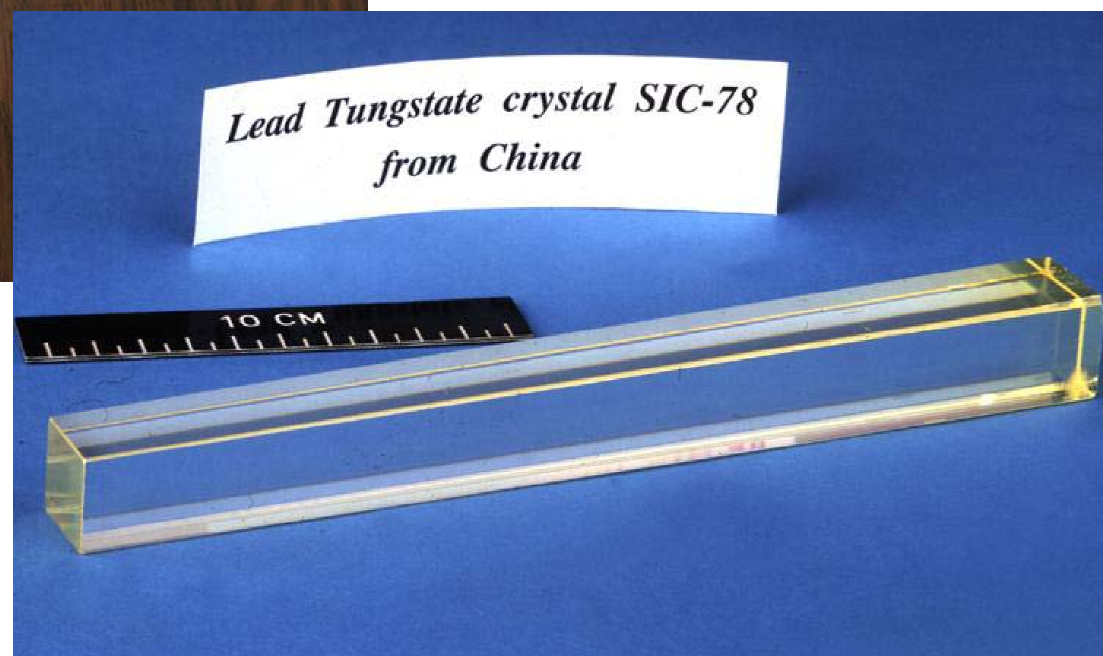

$PbWO_4$ ingot and final polished CMS ECAL scintillator crystal from Bogoroditsk Techno-Chemical Plant (Russia).

Inorganic Scintillators: NaI, BGO, $PbWO_4$, …

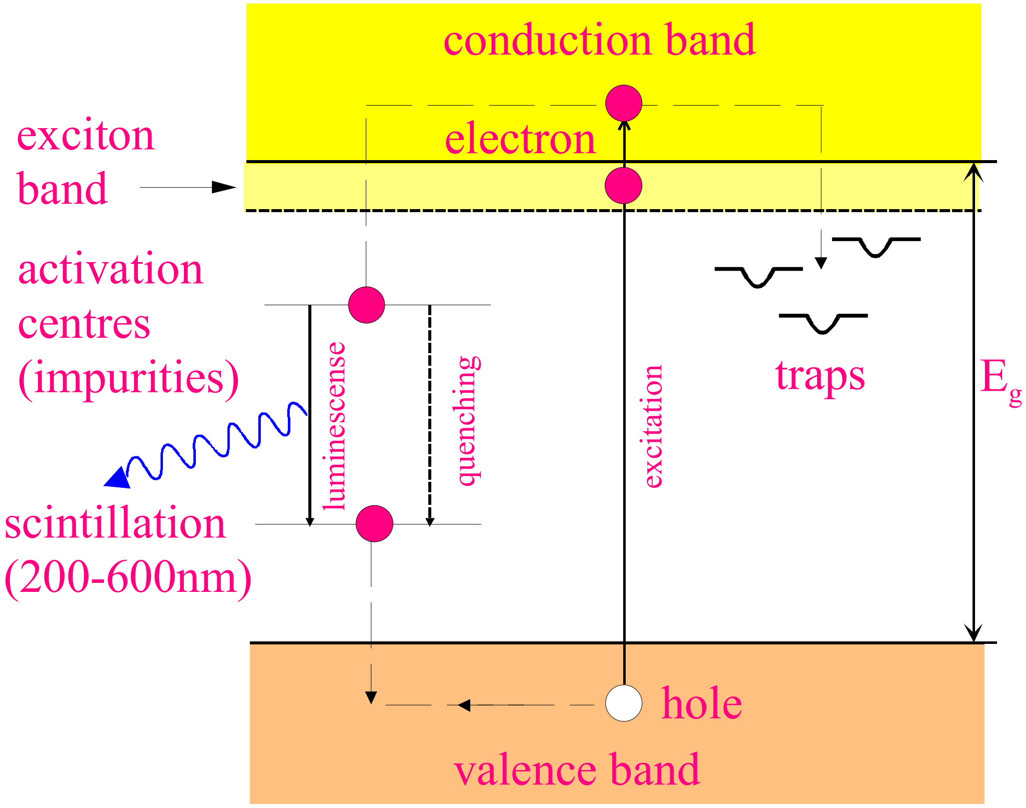

- Excitation of electrons into the conduction band allows light to be produced during relaxation to the ground state.
- Inorganic scintillators are usually high density and high Z materials
- Thus they can stop ionizing radiation in a short distance

Scintillation Light: Organic Scintillators

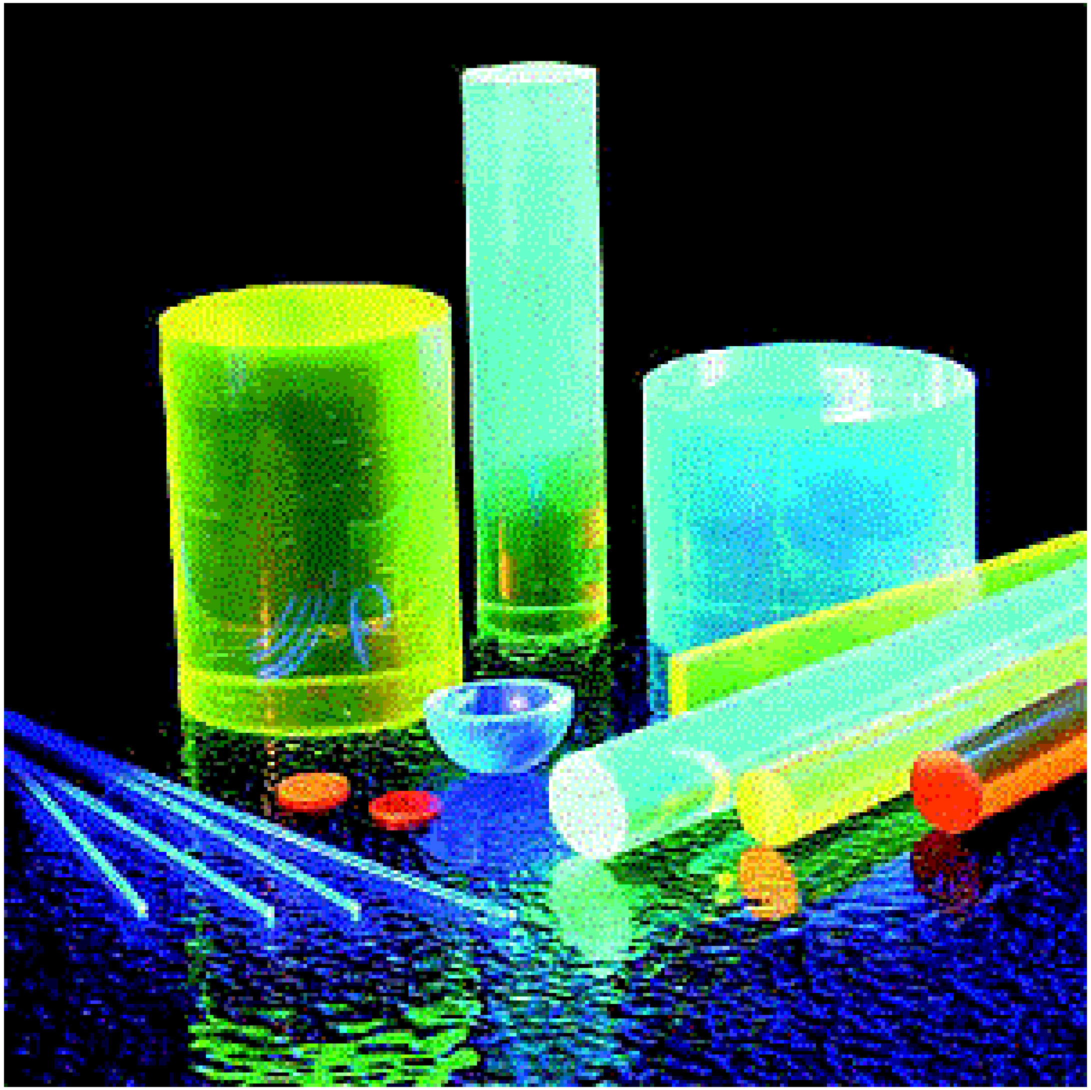

- Liquid and plastic organic scintillators are available
- They normally consist of a solvent plus secondary (and tertiary) fluors as wavelength shifters.

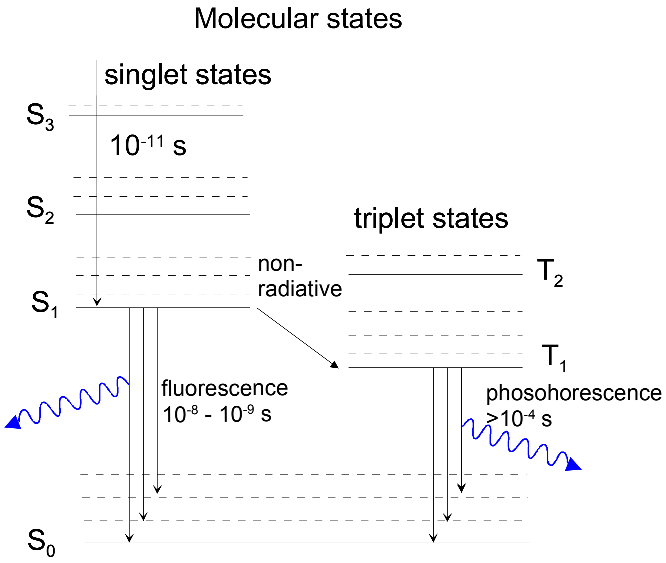

Geometrical adaptation:

Light guides: transfer by total internal reflection (+outer reflector)

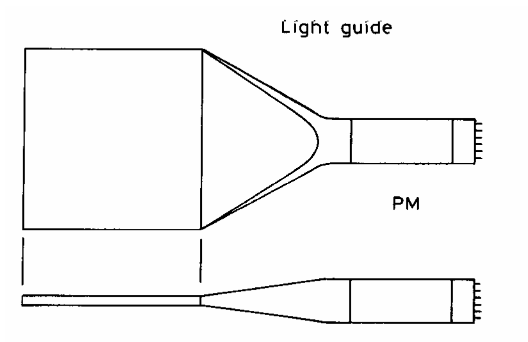

"fish tail"

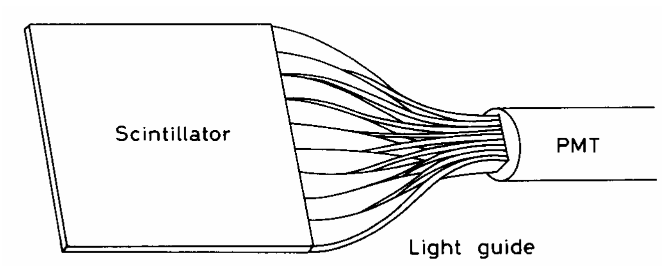

adiabatic

Wavelength shifter (WLS) bars

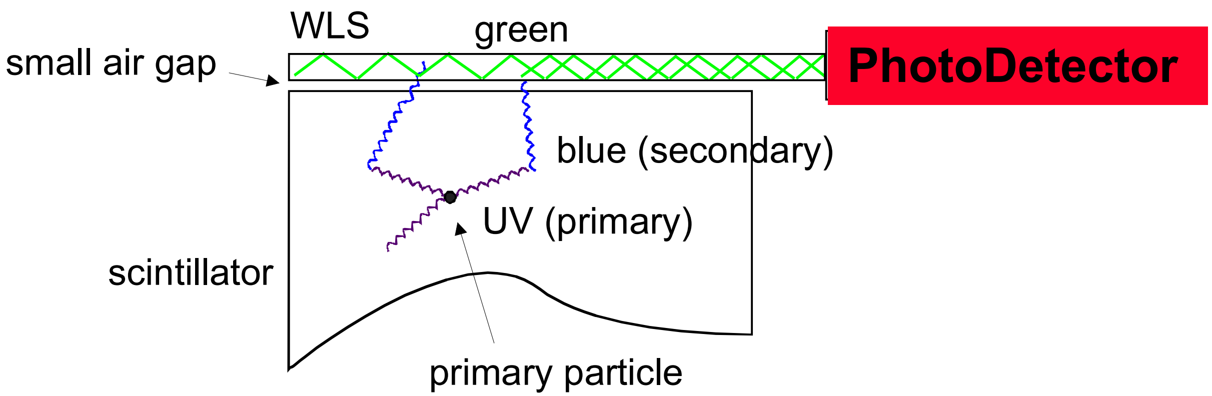

Photo Multiplier Tubes (PMT)

(Philips Photonic)

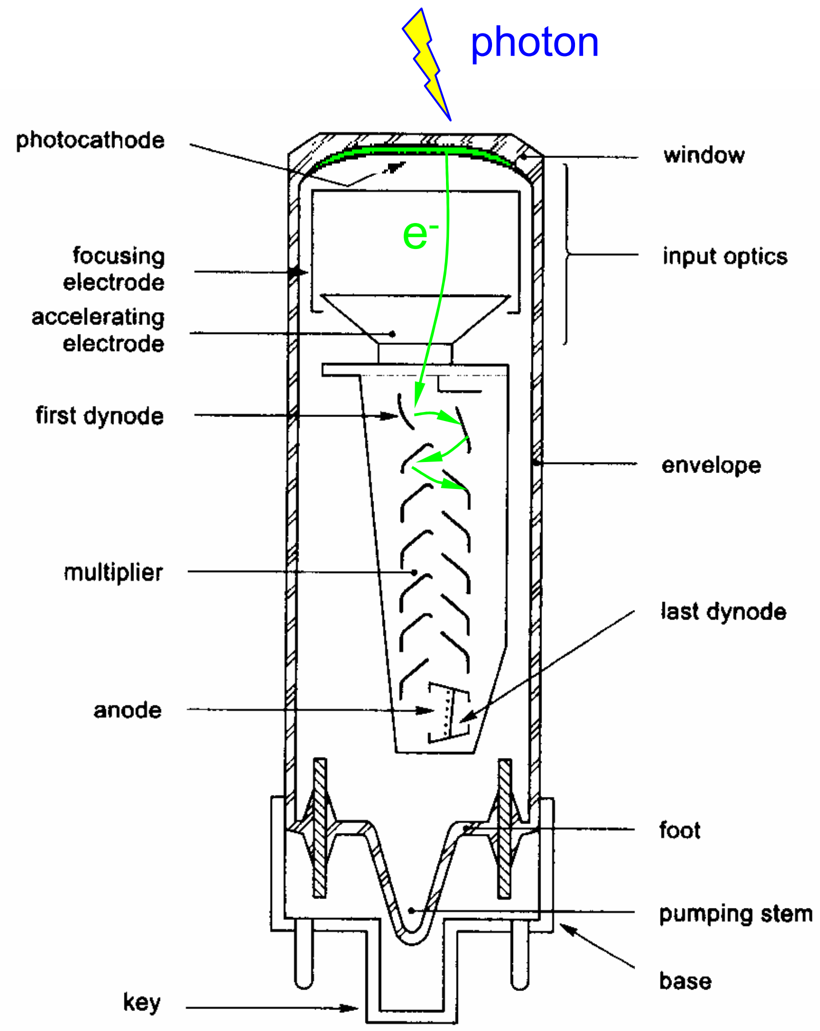

Main phenomena:

- photo emission from photo cathode.
- secondary emission from dynodes.
  dynode gain g = 3-50 (f(E))
- total gain
  10 dynodes with g=4
  $M = 4^{10} \approx 10^6$

Scintillator Applications

Tracking

Charged particle passing through a stack of scintillating fibers (diam. 1mm)

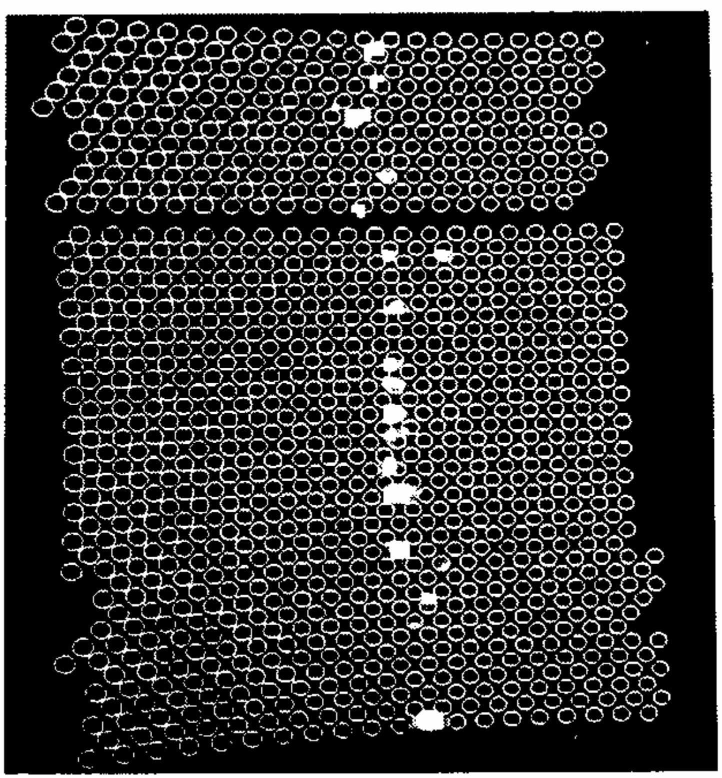

Sampling Calorimeters

Absorber + detector separated $\rightarrow$ additional sampling fluctuations

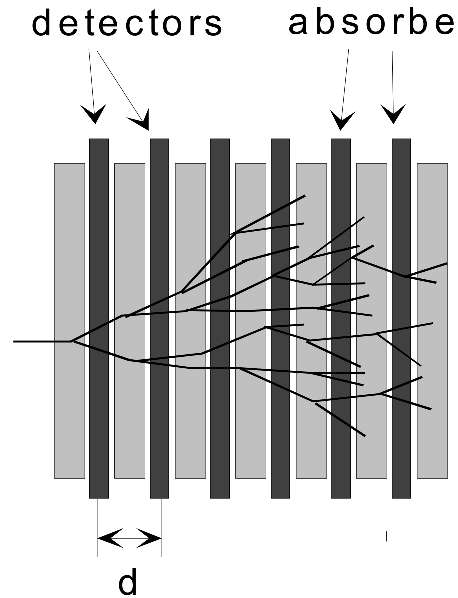

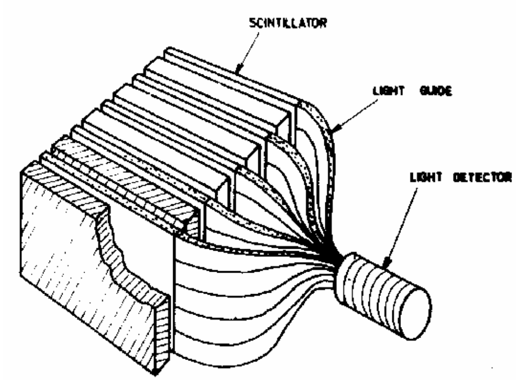

Time of Flight

Measure the time of flight of a particle between a thin, flat, “start” counter and a thin “stop” counter.

Measurement of Energy: Calorimeters

Neutral and charged particles incident on a block of material deposit their energy through destruction and creation processes

The deposited energy is rendered measurable by ionisation or excitation of the atoms of matter in the active medium.

The active medium can be the block itself *(totally active or homogeneous calorimeter)* or a sandwich of dense absorber and light active planes *(sampling calorimeters)*.

The measurable signal is usually linearly proportional to the incident energy.

Big European Bubble Chamber
filled with Ne:H_2 = 70%:30%
3T field, L=3.5m, X_0=34 cm
50 GeV incident electron

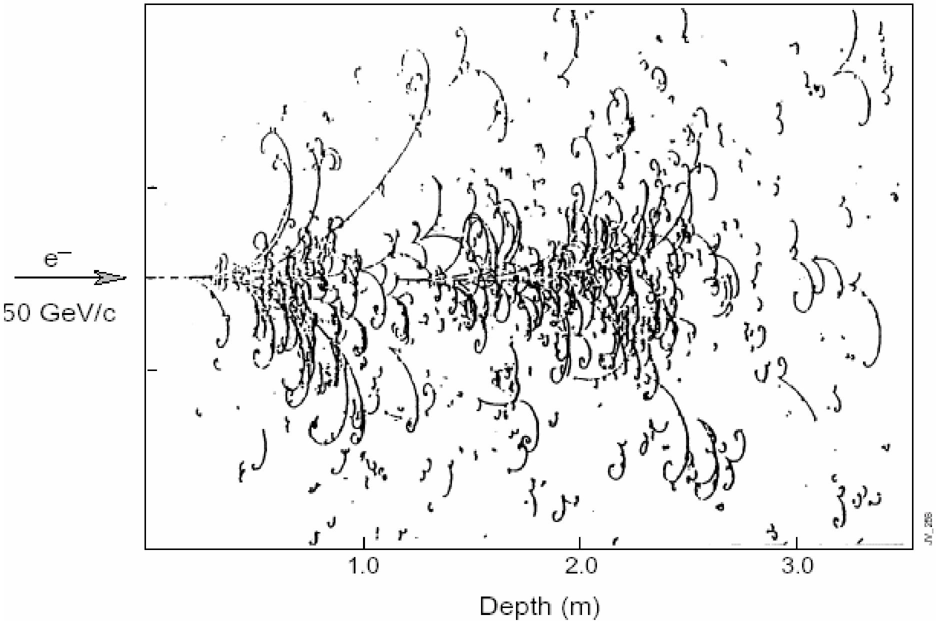

Electromagnetic Cascade

A high energy e or γ incident on a thick absorber initiates a cascade of $e^{\pm}$'s, γ's via bremstrahlung and pair production.

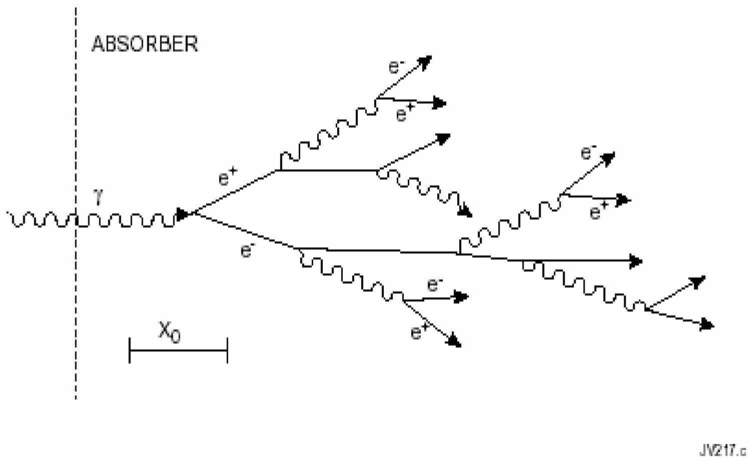

The multiplication continues until the energies fall below the critical energy ε.

Simplemodel of shower development - use scaled variables

$$t = \frac{x}{X_0} \quad and \quad y = \frac{E}{\varepsilon}$$

In 1 X_0, an electron loses about 2/3rd of its energy and a high energy photon has a probability of 7/9 of pair conversion - **naively take X_0 as a generation length**. Assume that after each generation the number of particles increases by a factor of 2.

Electromagnetic Cascade: Longitudinal Development

After t generations,

$$\text{energy of particles} \quad e(t) = \frac{E}{2^t}$$

$$\text{number of particles} \quad n(t) = 2^t$$

At shower max. where e ~ ε

$$\text{no. of particles} \quad n(t_{\max}) \approx \frac{E}{\varepsilon} = y$$

$$\text{and} \qquad t_{\max} \approx \ln\frac{E}{\varepsilon} = \ln y$$

After shower maximum

remaining energy is carried forward by photons giving the typical exponential falloff

Longitudinal Development EM Shower

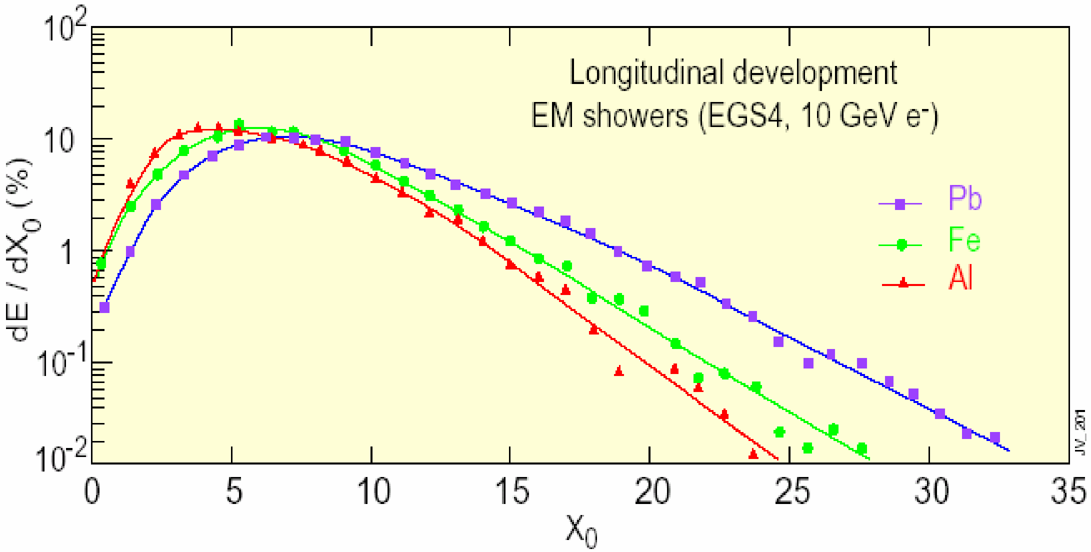

CSS99

Need a depth of > 25 X_0 to contain high energy em showers

Radiation Length and the Moliere Radius

Critical Energy, ε

Defined to be the energy at which the energy loss due to ionisation* (at its minimum i.e. β≈0.96) and radiation are equal (over many trials)

$$i.e.\quad \frac{(dE/dx)_{rad}}{(dE/dx)_{ion}} = 1$$

$$\Rightarrow \quad \varepsilon = \frac{560}{Z} \quad (E \;\; in \;\; MeV)$$

Fractional Energy Loss by Electrons

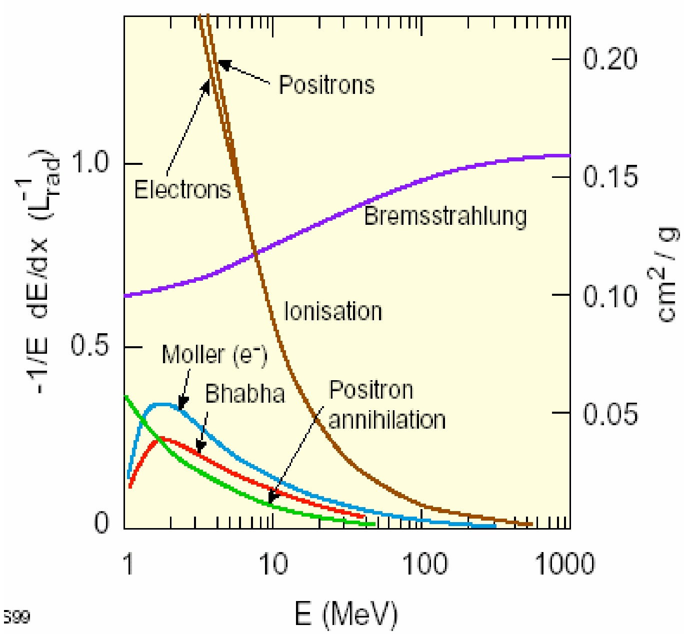

Moliere Radius, R_M

This gives the average lateral deflection of critical energy electrons after traversing 1 X_0 and can be parameterised as :

$$R_M = \frac{X_0 E_s}{\varepsilon} = \frac{21_{MeV} X_0}{\varepsilon} \approx \frac{7A}{Z} \quad g.cm^{-2}$$

	Z	ρ	I/Z	(1/ρ) dT/dx	X_0	ε	λint
		g.cm^{-3}	eV	MeV/g·cm^{-2}	cm	MeV	cm
C	6	2.2	12.3	1.85	~19	103	38.1
Al	13	2.7	12.3	1.63	8.9	47	39.4
Fe	26	7.87	10.7	1.49	1.76	24	16.8
Pb	82	11.35	10.0	1.14	0.56	6.9	15.1
U	92	18.7	9.56	1.10	0.32	6.2	10.5

$$-\frac{dE}{dx}\Big|_{rad} = \left[4n\,\frac{Z^2\alpha^3(\hbar c)^2}{m_e^2 c^4}\,\ln\frac{183}{Z^{1/3}}\right] E$$

* $$-\frac{dE}{dx}\Big|_{ion} = N_A\,\frac{Z}{A}\,\frac{4\pi\alpha^2(\hbar c)^2}{m_e c^2}\,\frac{Z_i^2}{\beta^2}\left[\ln\frac{2m_e c^2\gamma^2\beta^2}{I} - \beta^2 - \frac{\delta}{2}\right]$$

Hadronic Cascade

- Analogy with em showers. **Strong interaction** is responsible for shower development.
- A high energy hadron striking an absorber leads to multi-particle production consisting of mesons (e.g. $\pi^{\pm}$, π^{0}, K etc.). These in turn interact with further nuclei
- Nuclei breakup leading to spallation neutrons.
- Multiplication continues until the pion production threshold, $E_{th} \sim 2\ m_{\pi} = 0.28$ GeV

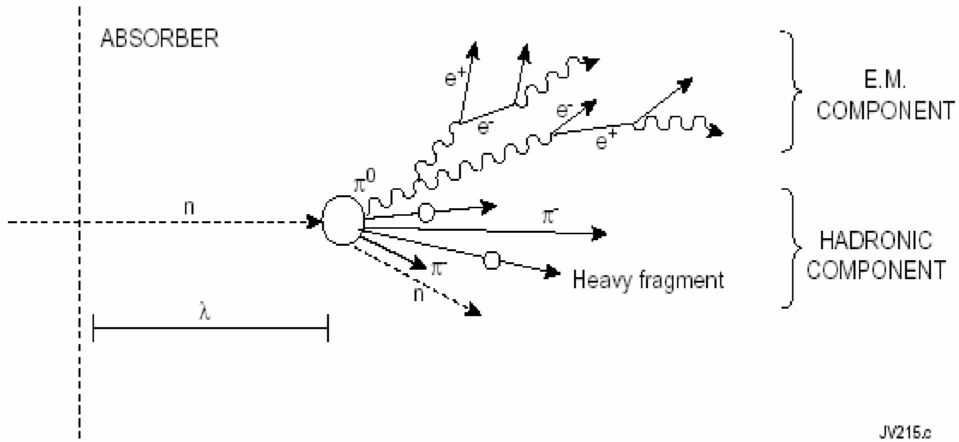

Simple model treats interaction on a black disc of radius R $\sigma_{int} = \pi R^2 \propto A^{2/3}$

Infact $\sigma_{inel} = \sigma_0 A^{0.7}$ where $\sigma_0 = 35$ mb

Defne nuclear interaction length $\lambda_{int} = \frac{A}{N_A \sigma_{int}} \propto A^{1/3}$ $\lambda \sim 35\ A^{1/3}$ g cm^{-2}

Cascade particles have a limited transverse momentum $\langle p_T \rangle \approx$ 300-400 MeV

150 GeV Pion Showers in Cu

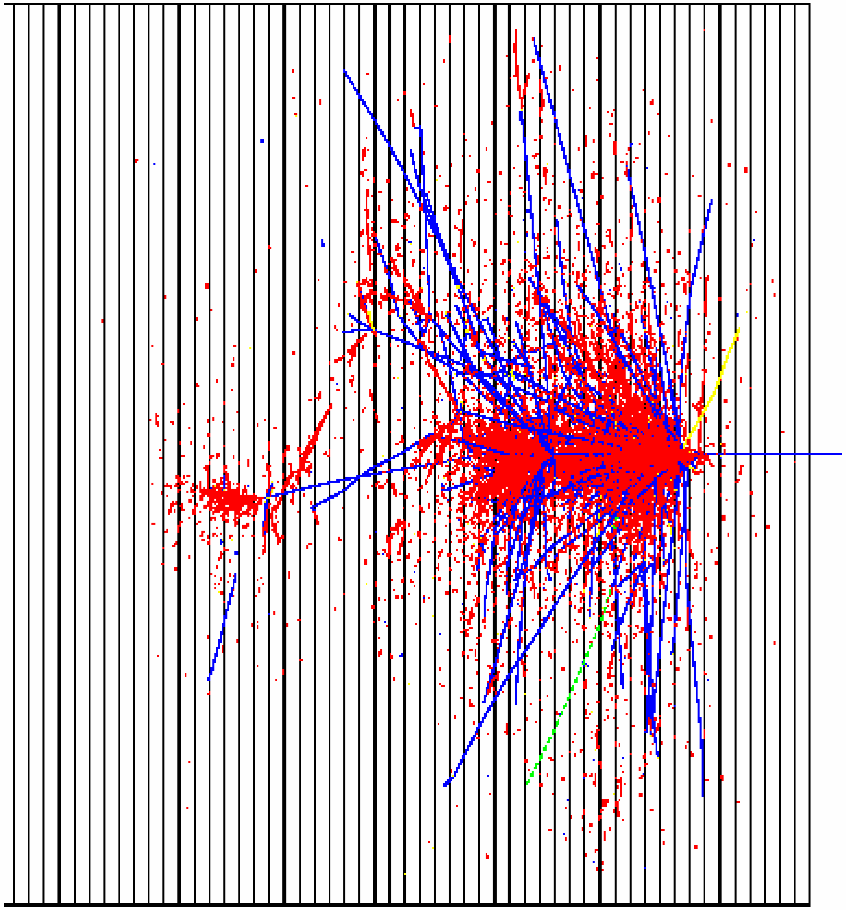

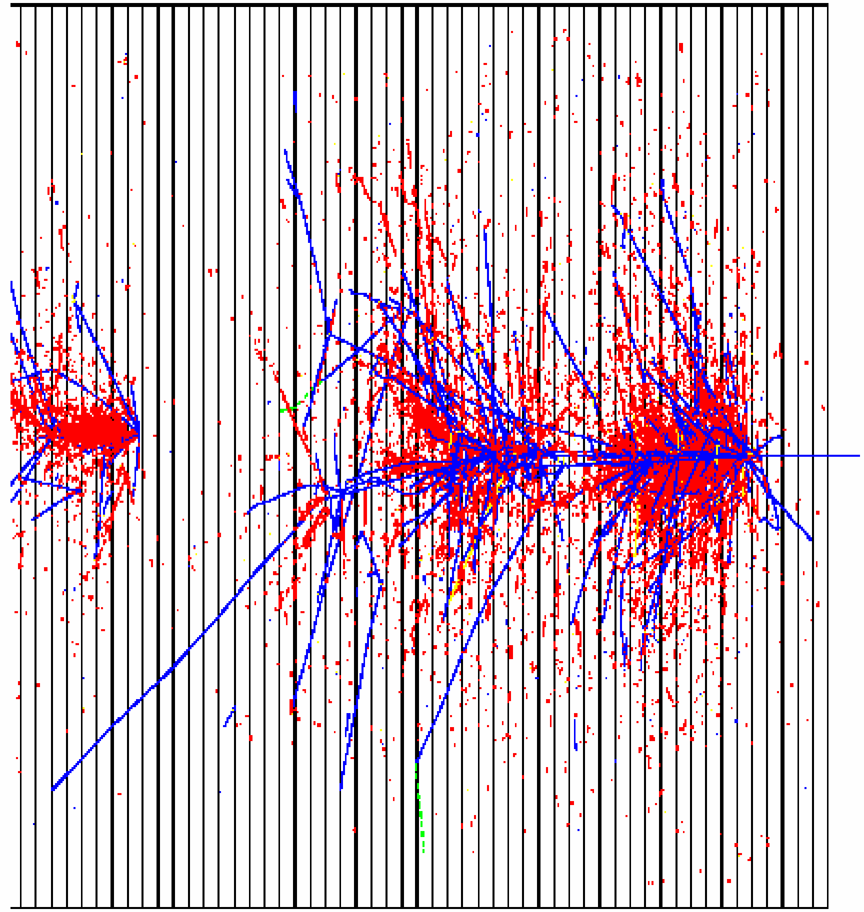

Hadron shower not as well behaved as an em one

red - e.m. component
blue - charged hadrons

Hadron calorimeter are always sampling calorimeters

Hadronic Cascade: Profiles

Hadron shower profiles for single $\pi^{\pm}$

Longitudinal

- sharp peak from π^0's produced in the 1st interaction
- followed by a more gradual falloff with a characteristic scale of λ.

WA78 : 5.4λ of 10mm U / 5mm Scint + 8λ of 25mm Fe / 5mm Scint

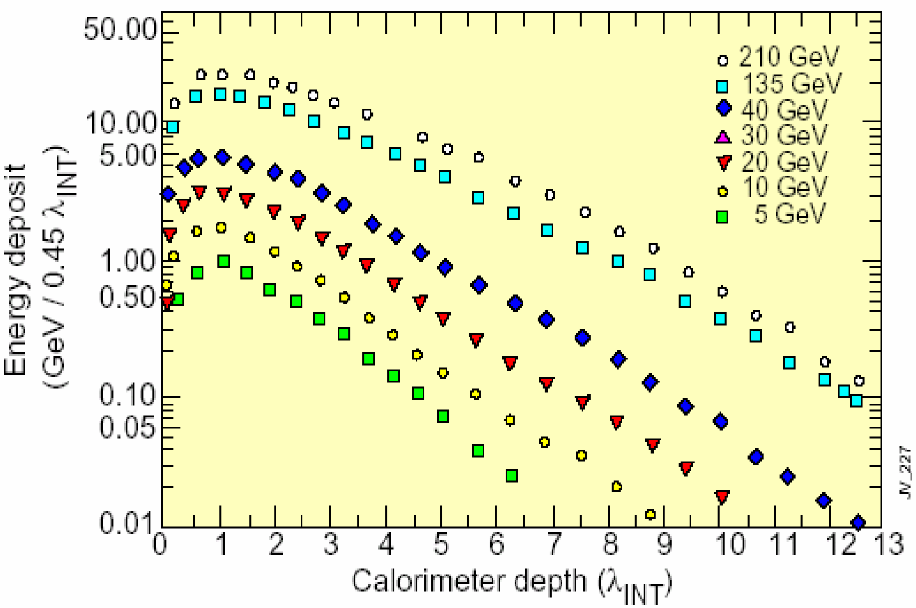

Approx. 10 λ required to contain 99% of the energy of $\approx$ 200 GeV pions

Lateral

- Secondaries produced with $\langle p_t \rangle$ ~ 300 MeV -approx. energy lost in $\approx$ 1 λ in most materials.
- Characteristic transverse scale is $r_\pi \approx \lambda$.
- Pronounced core, caused by the π^0 component,

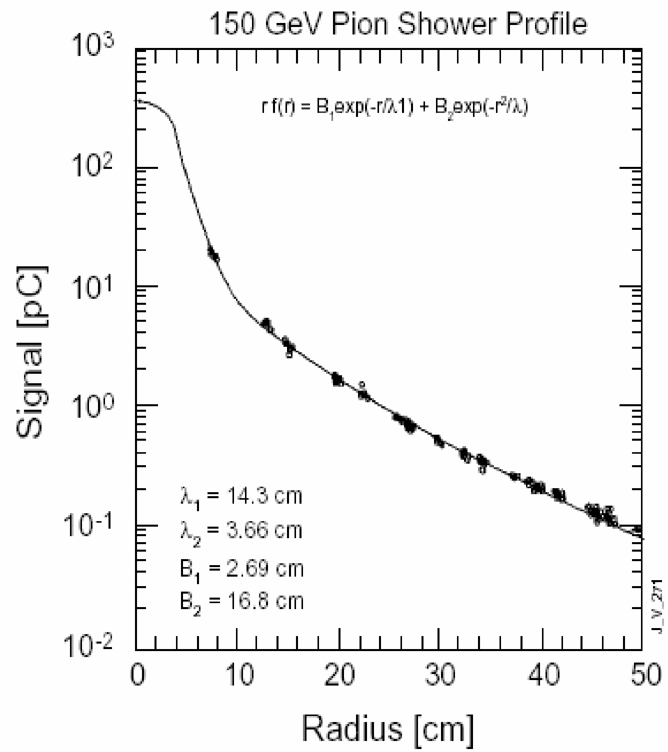

Transverse radius for 95% containment is $R_{0.95} \approx 1\ \lambda$

Lets Design a Detector: Requirements

Very good particle identification
trigger efficiently and measure ID and momentum of all particles

High resolution electromagnetic calorimetry

Powerful inner tracking systems
Improves momentum resolution, find tracks of short lived particles

Hermetic coverage
good rapidity coverage, good missing E_T resolution

Affordable detector

‘Cylindrical Onion-like’ Structure of HENP Detectors

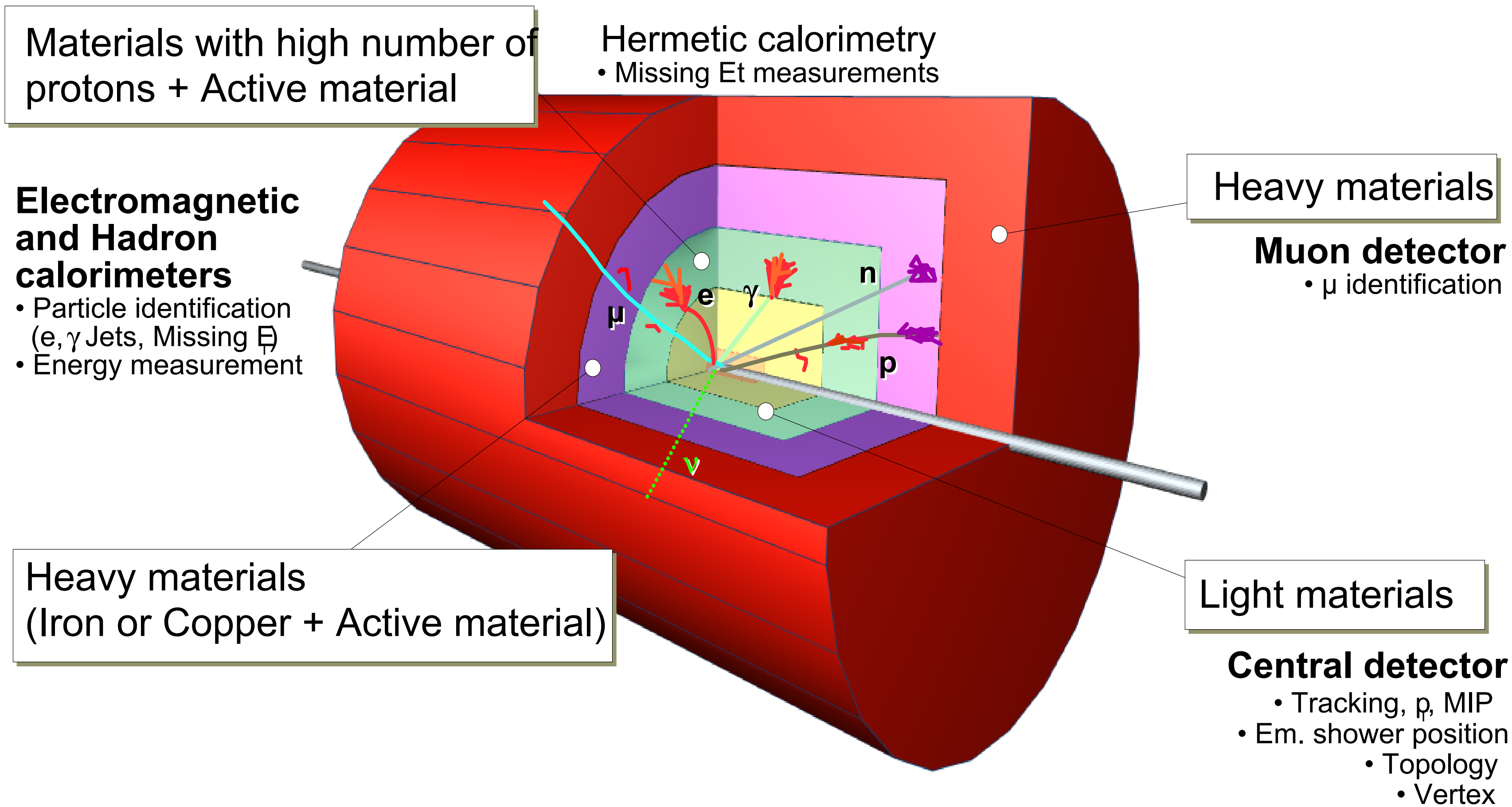

Each layer identifies and enables the measurement of the momentum or energy of the particles produced in a collision

The STAR Detector at RHIC

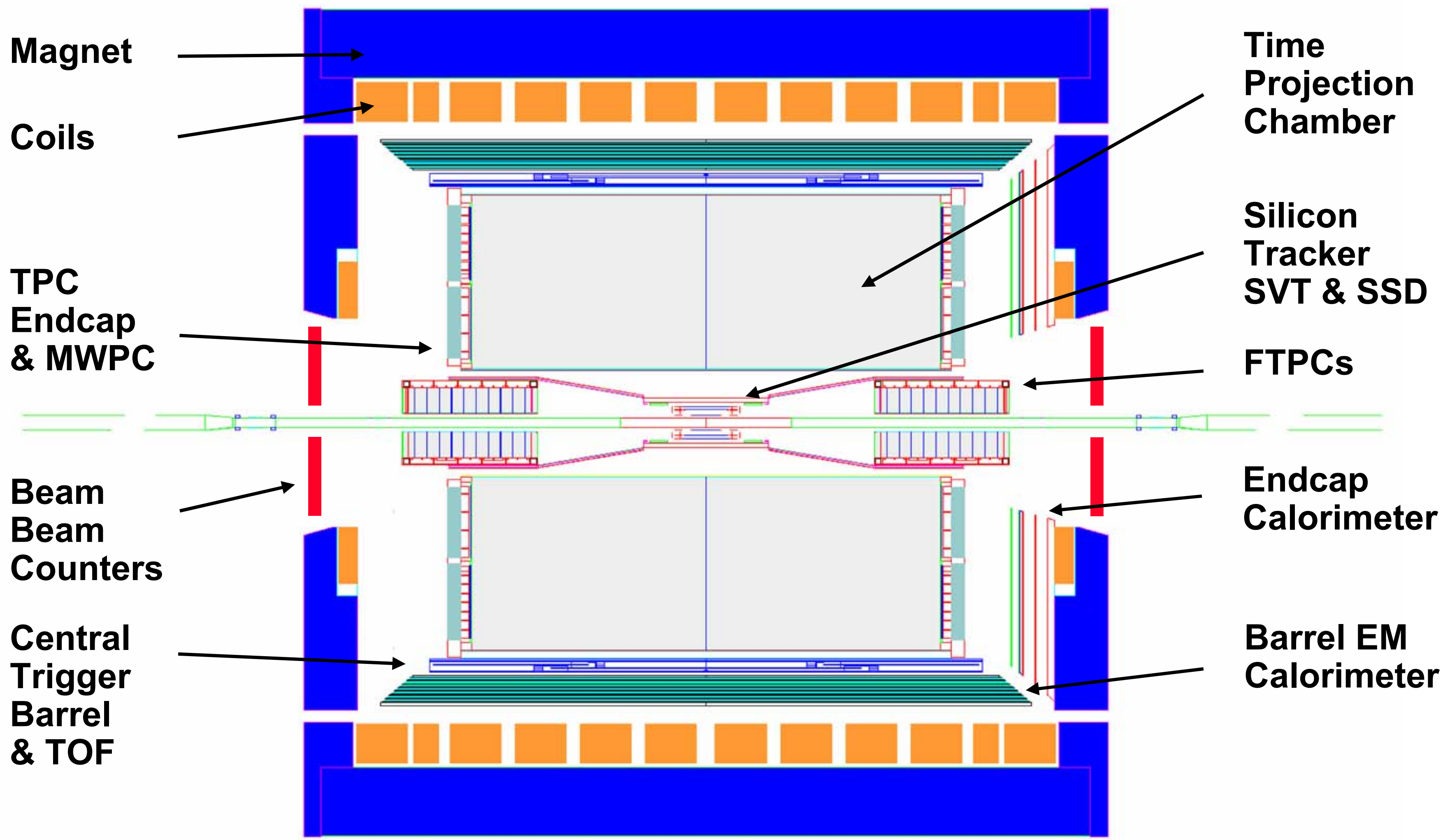

Not Shown: pVPDs, ZDCs, PMD, and FPDs

Conclusions

- We have taken a random walk through a variety of detector technologies and put the pieces together into a detector
- You can repeat this exercise using the PDG booklet (!)
  - It contains a wealth of information
  - It is extremely well written and only contains the most essential information
- The design of HENP detectors is driven by the desire to measure the ID and momentum of all particles in the range from 100 MeV to 100 GeV.
  - all 4 components of the momentum 4-vector (E, p_x, p_y, pz)
  - all 4 components of the spacial 4-vector (ct, x, y, z)
- If you can afford to do this with full 4π coverage, then your detector will end up looking pretty much like all the other big detectors. However, there are big differences in the details and cost effectiveness of each detector design.

Two "Large" Detectors at RHIC

STAR

Solenoidal field
Large Solid Angle Tracking
TPC's, Si-Vertex Tracking
RICH, EM Cal, TOF

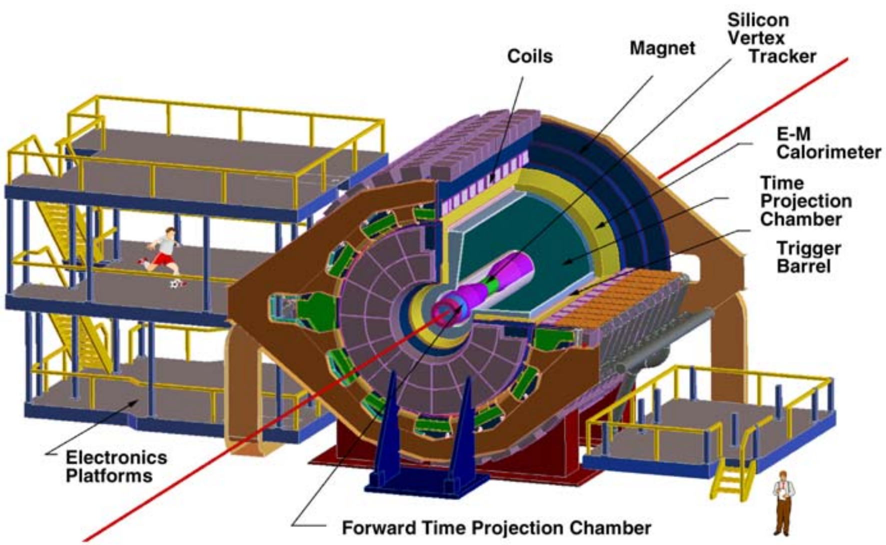

Measurements of <u>Hadronic</u> observables using a large acceptance spectrometer

Event-by-event analyses of global observables, hadronic spectra and jets

PHENIX

Axial Field
High Resolution & Rates
2 Central Arms, 2 Forward Arms
TEC, RICH, EM Cal, Si, TOF, μ-ID

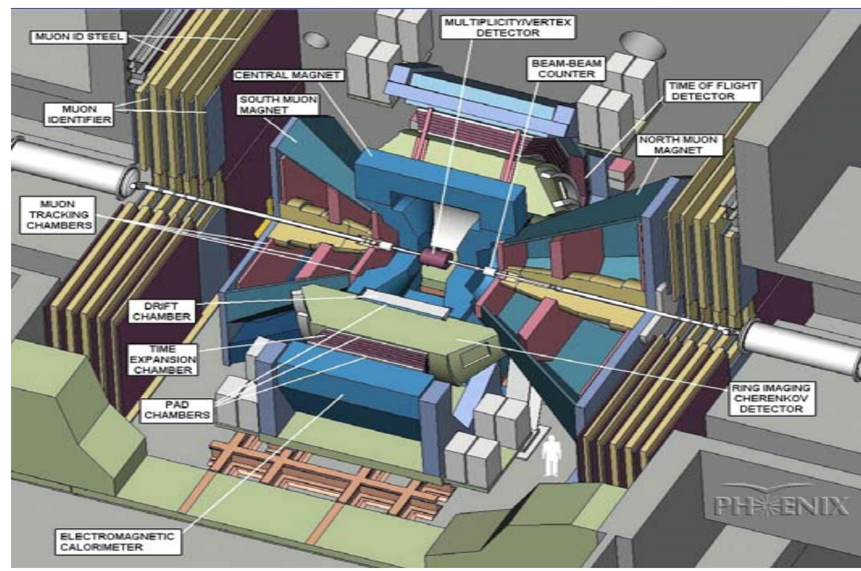

<u>Leptons</u>, Photons, and Hadrons in selected solid angles (especially muons)

Simultaneous detection of phase transition phenomena (e–μ coincidences)

Two “Small” Experiments at RHIC

BRAHMS

2 Spectrometers - fixed target geometry
Magnets, Tracking Chambers, TOF, RICH

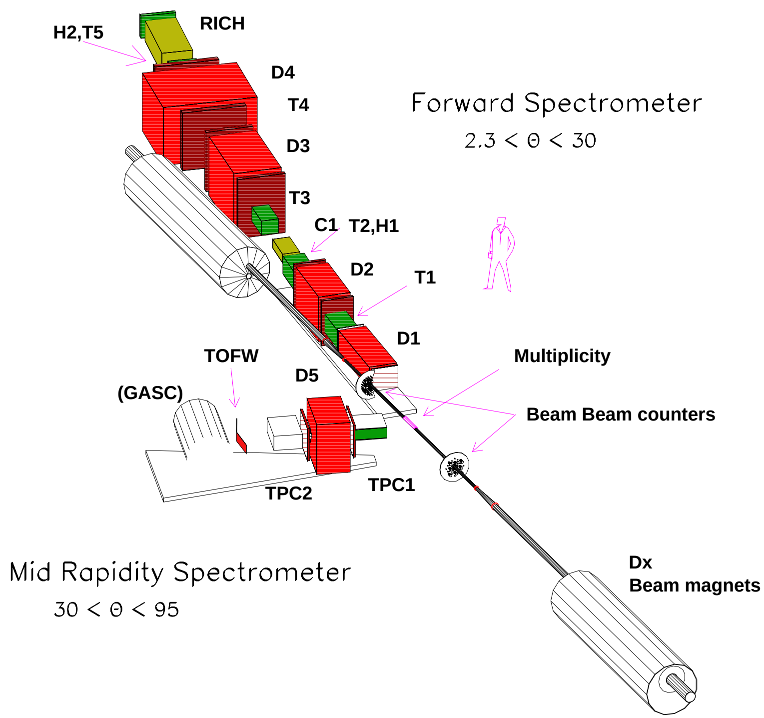

Inclusive particle production over a <u>large</u> rapidity and p_t range

PHOBOS

“Table-top” 2 Arm Spectrometer Magnet,
Si μ-Strips, Si Multiplicity Rings, TOF

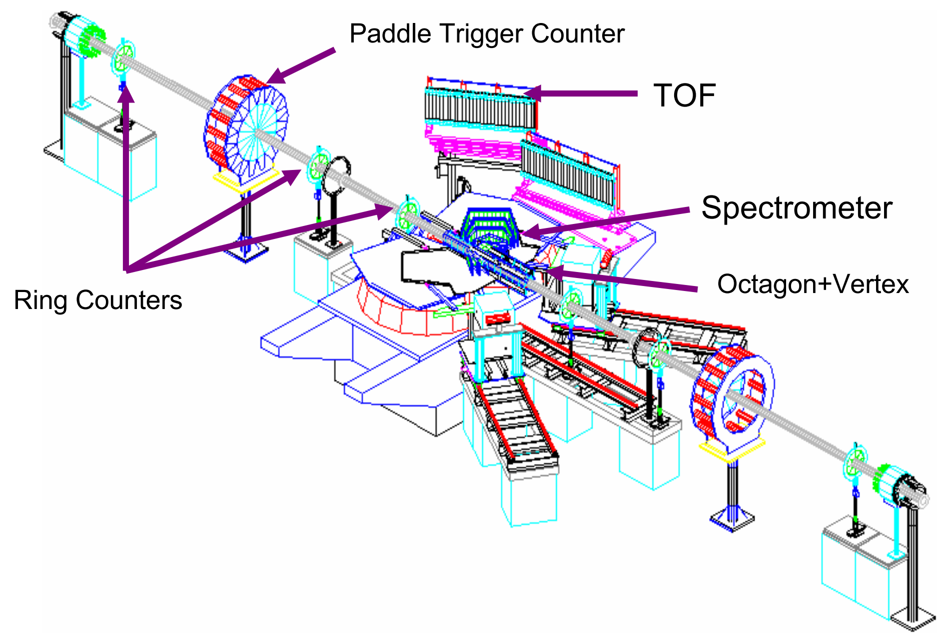

Low p_t charged hadrons
Multiplicity in 4π & Particle Correlations